

Renormalization and spectra of the Pöschl-Teller potential

Ulysses Camara da Silva^{*}

Carlos F.S. Pereira[†]

Universidade Federal do Espírito Santo – Departamento de Física

Av. Fernando Ferrari, Goiabeiras, 29075-900, Vitória-ES, Brasil

Andre Alves Lima[‡]

Universidade Federal de Pernambuco – Departamento de Física

Av. Professor Luiz Freire, Cidade Universitária, 50670-901, Recife-PE, Brasil

August 10, 2023

Abstract

We study the energy eigenfunctions and spectrum of the Pöschl-Teller potential for every value of its two dimensionless parameters. The potential has a singularity at the origin which, in some regions of parameter space, makes boundary conditions of the eigenfunctions ill-defined. We apply a renormalization procedure to obtain a family of well-defined solutions, and study the associated renormalization group (RG) flow. Renormalization introduces an anomalous length scale by “dimensional transmutation”. In the regions of coupling space where this scale cannot be set to zero, it spontaneously breaks the asymptotic conformal symmetry near the singularity. The symmetry is also explicitly broken by a dimensionful parameter in the potential. The existence of these two competing ways of breaking conformal symmetry gives the RG flow an interesting structure. We show that supersymmetry of the potential, when present, allows one to prevent spontaneous breaking of the asymptotic conformal symmetry. We use the family of eigenfunctions to compute the S-matrix in all regions of parameter space, for any value of anomalous scale. Then we systematically study the poles of the S-matrix to classify all bound, anti-bound and metastable states.

Keywords: Pöschl-Teller potential; Inverse-square singularity renormalization; Renormalization group flow; S-matrix; Supersymmetric quantum mechanics.

^{*}ulyssescamara@gmail.com

[†]carlos.f.pereira@edu.ufes.br

[‡]alves.lima@ufpe.br

Contents

1	Introduction	1
2	Boundary conditions and coupling space	4
2.1	The regions of coupling space	5
2.2	Supersymmetry and boundary conditions in the weak-medium region	7
3	The renormalization group of the Pöschl-Teller potential	9
3.1	Renormalization	9
3.2	Breaking of asymptotic conformal symmetry	11
3.2.1	Spontaneous and explicit symmetry breaking	12
3.2.2	RG flows without spontaneous symmetry breaking	13
3.2.3	The critical line $\nu = 0$	15
3.2.4	Strongly attractive coupling and the phase θ	16
4	Spectra of the Pöschl-Teller Hamiltonian	17
4.1	Spectrum at arbitrary L or θ	19
4.1.1	The medium-weak region	20
4.1.2	The strongly attractive region	21
4.2	Spectrum at the IR fixed point	22
4.3	Spectrum at the UV fixed point	25
4.4	Completing the spectrum in the medium-weak region	27
5	Conclusion	29
A	α-corrections to the running coupling	30
B	The critical line $g_s = -\frac{1}{4}$	32

1 Introduction

The Pöschl-Teller potential [1] is one of the rare exactly solvable potentials in quantum mechanics. We can write it in its general form with a convenient parametrization,

$$V(x) = \frac{2m\alpha^2}{\hbar^2} \left(\frac{g_s}{\sinh^2(\alpha x)} + \frac{g_c}{\cosh^2(\alpha x)} \right) \quad (1.1)$$

where m has units of mass, such that the energy eigenstates of a particle of mass m is determined by α , g_s and g_c . While α only sets a length scale $1/\alpha$, different combinations of the dimensionless couplings g_s and g_c can change the shape of $V(x)$ significantly, and have important consequences for the nature of the energy spectrum.

If $g_s \neq 0$, the potential is singular at $x = 0$, hence its eigenfunctions are defined only on half the real line, which we take to be $x > 0$. Near the singularity, we find asymptotic conformal symmetry [2, 3], as the Pöschl-Teller potential becomes the conformal potential, $V(x) \sim g_s/x^2$. It is well-known that the Hamiltonian of the conformal potential is a subtle operator, with very distinct mathematical and physical properties, depending on the value of g_s : we can divide its one dimensional ‘coupling space’ into three regions:

- i) $\frac{3}{4} < g_s$, where the potential is ‘strongly repulsive’;
- ii) $-\frac{1}{4} \leq g_s < \frac{3}{4}$, where the potential is ‘medium-weak’;
- iii) $g_s < -\frac{1}{4}$, where the potential is ‘strongly attractive’.

Square-integrability of eigenfunctions is a well-defined boundary condition at $x = 0$ only if g_s is in the strongly repulsive region. In the other two regions, the Hamiltonian is not self-adjoint, the boundary conditions become ambiguous, and the problem must be carefully examined. Construction of the self-adjoint extension produces one-parameter families of eigenfunctions, well-defined in all three regions [4]. The Pöschl-Teller potential (1.1) inherits these subtleties of the conformal potential, but its coupling space is a two-dimensional g_c - g_s plane. Because of the boundary conditions at the origin, the plane is divided into three sections across the g_s -axis, corresponding to “strongly repulsive”, “medium-weak” and “strongly attractive”, as in the conformal case. In the direction of the g_c -axis, we also have a dividing line, which determines if (1.1) is supersymmetric or not.

Although the work of Herta Pöschl and Edward Teller [1] is now centenary, the Pöschl-Teller potential is relevant in many modern applications, such as linear perturbations of relativistic kinks [5–9], of de Sitter spacetime [10], and as an important tool for the computation of black hole quasinormal modes [11–16].

In this paper, we will compute the eigenfunctions of the Pöschl-Teller Hamiltonian in all regions of parameter space. We will deal with boundary conditions at the singularity by applying a *renormalization procedure*, like the one developed for the inverse-square potential [17–22]. As in the self-adjoint extension construction [4], the result is a one-parameter family of eigenfunctions, but the renormalization group (RG) approach provides clear interpretation of that parameter, as a length scale L that appears by “dimensional transmutation” [23], and breaks conformal symmetry.

The RG flow of the Pöschl-Teller is crucially different from that of the exact conformal potential because of the dimensionful parameter α in (1.1). While the anomalous scale L causes the asymptotic conformal symmetry to be *spontaneously* broken, the length scale $1/\alpha$ *explicitly* breaks it. The hierarchy between L and $1/\alpha$ enriches the RG structure. In general, it is not possible to separate the effect of each scale in the breaking of conformal symmetry, but in certain cases when one scale is much larger than the other we can have a “competition” between which one breaks conformal symmetry “first”.

We can characterize the breaking of asymptotic conformal symmetry by defining a dimensionless running coupling $\gamma(R)$, analogous to the one defined for the conformal case

[19, 22, 24, 25], as a function of the distance cutoff R near the singularity of (1.1). This coupling has an associated beta function, and an RG flow, with a UV fixed point at $R = 0$. For R sufficiently small, the beta function coincides with the one of the conformal inverse-square potential. If the anomalous scale L is finite, but much smaller than the ‘classical’ length scale $1/\alpha$, the asymptotic conformal symmetry is spontaneously broken much before $1/\alpha$ has the chance of explicitly breaking it. This can affect the spectrum of the Hamiltonian, allowing the existence of new bound states that were previously forbidden.

Spontaneous breaking of asymptotic conformal symmetric can be fully prevented if the anomalous scale is set to $L = 0$ or $L = \infty$. Then, the symmetry is only broken explicitly, by the scale $1/\alpha$. We will show that these two cases give rise to a pair of new beta functions, which cannot be perturbatively derived from the conformal beta function. Each describe a different type of massive RG flow with a UV fixed point at $R = 0$, and a mass scale set by α .

In the strongly repulsive region *i*) of the parameter plane g_c - g_s , we are forced to fix the anomalous scale $L = 0$. This is imposed by normalizability of the wave function at $x = 0$, and prevents the asymptotic symmetry from being spontaneously broken. We will show that, in a certain patch of the medium-weak region, we can use supersymmetry (SUSY) to fix $L = 0$ as well. In quantum mechanics, a potential is supersymmetric if it can be written in a specific way in terms of a ‘superpotential’ [26]. When this is the case, SUSY relates the Hamiltonian to a partner whose potential is, in general, very different, but the spectrum of the pair is (essentially) the same. In special cases, the superpartner potentials are *the same* function, and the potential is said to be ‘shape invariant’ [26, 27]. For some regions in the g_c - g_s plane, the Pöschl-Teller potential has SUSY and, moreover, is shape invariant. More precisely, given (1.1) with g_s in (part of) the strongly repulsive region, its superpartner is again (1.1), but with a different g_s , now in the weak-medium region. We will show how imposing SUSY fixes $L = 0$ in the patch of the weak-medium region where there is otherwise no reason for not leaving L arbitrary. This phenomenon is analogous to the one described in [25] for the conformal potential.

Finally, once we have the energy eigenfunctions parameterized by the anomalous dimension, we proceed to investigate the spectra of the Pöschl-Teller Hamiltonian, in every region of its coupling space. As said before, spontaneous breaking of conformal symmetry may affect the spectrum, creating bound states where the conformal invariance would otherwise forbid them. To study the spectrum, we compute the S-matrix over the entire coupling plane. Then, from a systematic analysis of its poles, we determine the spectra of bound, anti-bound and metastable states.

The structure of this paper is as follows. In Sect.2 we describe the coupling plane g_c - g_s with its qualitatively different regions, and the problem of boundary conditions at the singularity. We examine in which regions the Pöschl-Teller potential is supersymmetric, and how SUSY and shape-invariance can be used to fix the ill-defined boundary conditions for certain ranges of the couplings. In Sect.3, we first apply the renormalization procedure to

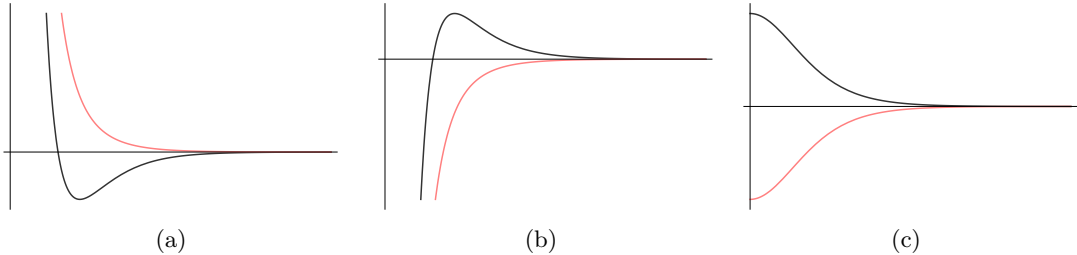


Figure 1: Shapes of $\mathcal{V}(x)$.

- (a) $g_s > 0$. Black: $g_c < 0$ and $g_s/|g_c| < 1$. Red: $g_s/|g_c| > 1$.
- (b) $g_s < 0$. Black: $g_c > 0$ and $|g_s|/g_c < 1$. Red: $|g_s|/g_c > 1$.
- (c) $g_s = 0$. Black: $g_c > 0$. Red line: $g_c < 0$.

obtain the general family of energy eigenfunctions, parameterized by an anomalous scale. Then, we define the renormalization group with a running coupling and the associated beta function. In this framework, we study how the asymptotic conformal symmetry of the Pöschl-Teller potential is broken, either spontaneously, by the anomalous dimension, or explicitly, by the length scale $1/\alpha$. In Sect.4, we compute the S-matrix for the potential in all generality, and systematically search for bound, anti-bound and metastable states, and instabilities in all regions of parameter space. In Sect.5 we make our concluding remarks. Details of some computations are given in Appendices A and B.

2 Boundary conditions and coupling space

Let us define the rescaled Pöschl-Teller potential

$$\mathcal{V}(x) = \alpha^2 \left(\frac{g_s}{\sinh^2(\alpha x)} + \frac{g_c}{\cosh^2(\alpha x)} \right), \quad 0 < x < \infty, \quad (2.1)$$

related to (1.1) by $\mathcal{V}(x) = 2m\hbar^{-2}V(x)$. Here $\alpha > 0$ has dimension of inverse length and does not affect the shape of \mathcal{V} . Our concern will be the two dimensionless couplings g_s and g_c , which define a two-dimensional ‘coupling space’. As we will show, in different regions of the coupling plane, the properties of the potential and its spectrum can be very distinct. First of all, $\mathcal{V}(x)$ has qualitatively distinct shapes, depending on how the couplings g_c and g_s are chosen, as shown in Fig.1, from which it is clear that different shapes of $\mathcal{V}(x)$ may support or not bound states.

We have chosen the normalization of (2.1) such that the stationary Schrödinger equation reads

$$\frac{d^2\psi(x)}{dx^2} + [k^2 - \mathcal{V}(x)]\psi(x) = 0, \quad k = \sqrt{2mE/\hbar}. \quad (2.2)$$

For now, we will take $k \in \mathbb{C}$ to be arbitrary, and consider specific values of interest later. The goal is to first find the general solution of Eq.(2.2). Defining $u = \tanh^2(\alpha x)$, $0 < u < 1$, the Schrödinger equation becomes

$$u(1-u) \frac{d^2\psi(u)}{du^2} + \left(\frac{1}{2} - \frac{3}{2}u\right) \frac{d\psi(u)}{du} + \left(\frac{1}{(1-u)} \frac{k^2}{4\alpha^2} - \frac{1}{u} \frac{g_s}{4} - \frac{g_c}{4}\right) \psi(u) = 0. \quad (2.3)$$

The general solution can be written as

$$\psi_k(x) = [\tanh(\alpha x)]^{\frac{1}{2}+\nu} [\cosh(\alpha x)]^{-i\frac{k}{\alpha}} F(x), \quad (2.4a)$$

where $F(x)$ is a combination of hypergeometric functions,

$$\begin{aligned} F(x) = & \frac{A_k}{\alpha^{\frac{1}{2}+\nu}} {}_2F_1 \left[\frac{1}{2}(1+\nu-\mu+ik/\alpha), \frac{1}{2}(1+\nu+\mu+ik/\alpha); 1+\nu; \tanh^2(\alpha x) \right] \\ & + \frac{B_k}{\alpha^{\frac{1}{2}-\nu}} \frac{1}{\tanh^{2\nu}(\alpha x)} {}_2F_1 \left[\frac{1}{2}(1-\nu-\mu+ik/\alpha), \frac{1}{2}(1-\nu+\mu+ik/\alpha); 1-\nu; \tanh^2(\alpha x) \right] \end{aligned} \quad (2.4b)$$

and we have defined

$$\nu = \sqrt{\frac{1}{4} + g_s}, \quad \mu = \sqrt{\frac{1}{4} - g_c}. \quad (2.5)$$

The solution (2.4) is not valid if $\nu \in \mathbb{Z}_{\geq 0}$, but after analyzing boundary conditions at $x = 0$ we find that only non-trivial case is when $\nu = 0$, i.e. $g_s = -1/4$. In this case there is a logarithmic branch cut, as discussed in Appendix B. Unless specified, we will assume that $\nu \neq 0$.

2.1 The regions of coupling space

The parameters μ , ν defined in (2.5) can be used instead of g_s and g_c to describe the coupling space,

$$\begin{aligned} \nu &= \sqrt{\frac{1}{4} + g_s}, & g_s &= -\frac{1}{4} + \nu^2, \\ \mu &= \sqrt{\frac{1}{4} - g_c}, & g_c &= +\frac{1}{4} - \mu^2. \end{aligned} \quad (2.6)$$

In fact, many of the features that we will explore are more naturally described in terms of μ and ν , instead of g_c and g_s .

The parameters μ and ν relate directly to properties of the eigenfunctions. Their behavior near the singularity is controlled by the value of ν , and behavior at infinity by the value of μ . Either one of ν and μ may be real or purely imaginary, and the lines $g_s = -\frac{1}{4}$ and $g_c = \frac{1}{4}$, where they change from real to imaginary define the boundaries of regions in the coupling plane where the Pöschl-Teller system changes qualitatively. In the end, the coupling plane can be divided into six semi-infinite regions, represented in Fig.2.

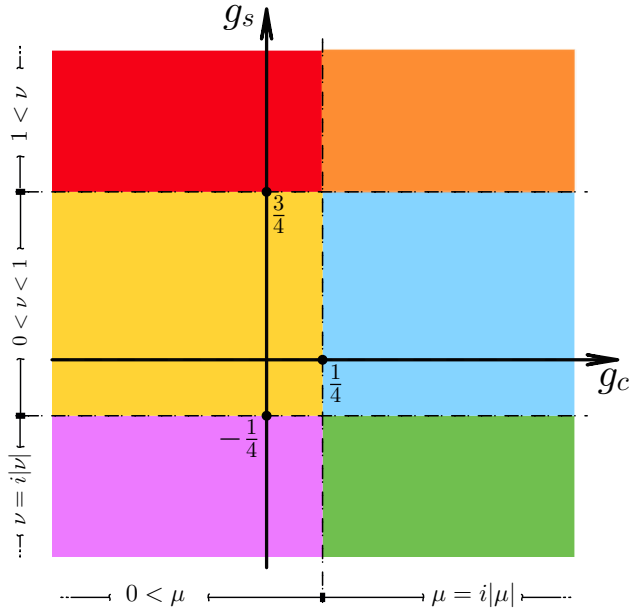


Figure 2: Coupling space, and its regions. Red and orange patches: strongly repulsive region. Yellow and blue: weak medium. Purple and green: strongly attractive. The vertical line $g_c = \frac{1}{4}$ marks the division between real and imaginary μ .

The three different regions across the horizontal g_s -axis in Fig.2 correspond to the three possible behaviors of the solutions near the singularity. The constants A and B in (2.4) are chosen such that the asymptotic solution near the origin looks simple. Expanding the hypergeometrics for $\alpha x \ll 1$, we find that, if $g_s > -\frac{1}{4}$, hence ν is real, then

$$\psi_k(x) \approx x^{1/2} [A_k x^\nu + B_k x^{-\nu}]. \quad (2.7a)$$

This is the behavior in the red, orange, yellow and blue patches of Fig.2. On the remaining purple and green patches, $g_s < -\frac{1}{4}$, hence $\nu = i|\nu|$ is imaginary, and

$$\psi_k(x) \approx x^{1/2} \left[A_k x^{i|\nu|} + B_k x^{-i|\nu|} \right], \quad A_k = B_k^* \quad (2.7b)$$

The constants A and B must be complex conjugates, so that $\psi_k(x)$ is real, since this is the solution of a real ODE.

The solution must be square-integrable near the singular point,

$$\lim_{x \rightarrow 0} \int^x |\psi_k(x')|^2 dx' < \infty. \quad (2.8)$$

From the asymptotic forms (2.7), we find three distinct possibilities.

- i) If $g_s \geq \frac{3}{4}$, hence $\nu \geq 1$, condition (2.8) fixes $B = 0$ in Eq.(2.7a). In parameter space, this region is made by the (infinite) red and orange patches shown in Fig.2. Following nomenclature from the conformal potential literature, we will say that these patches form the “strongly repulsive region”.
- ii) If $-\frac{1}{4} \leq g_s < \frac{3}{4}$, hence $0 \leq \nu < 1$, both x^ν and $x^{-\nu}$ are square-integrable. Then condition (2.8) does *not* fix any of the constants A or B in Eq.(2.7a). These conditions are met at the yellow and blue patches of Fig.2, which we will call the “weak medium” region in coupling space.
- iii) If $g_s < -\frac{1}{4}$, hence $\nu = i|\nu|$, the solution is (2.7b), which is strongly oscillating as $x \rightarrow 0$. This holds in the purple and green patches of Fig.2, which form the “strongly attractive region” of coupling space.

The ambiguity in boundary conditions in cases *ii*) and *iii*) mean that the conformal Hamiltonian is not self-adjoint for $g_s < \frac{3}{4}$ [4].

2.2 Supersymmetry and boundary conditions in the weak-medium region

Two Hamiltonians H_\pm are a ‘supersymmetric’ pair if they can be factorized as a products of the conjugate operators¹

$$Q = \frac{d}{dx} + W(x), \quad Q^\dagger = -\frac{d}{dx} + W(x), \quad (2.9)$$

defined by a (real) ‘superpotential’ function $W(x)$, such that [26]

$$\begin{aligned} H_+ &= Q^\dagger Q = -d^2/dx^2 + U_+(x) & U_+(x) &= W^2(x) - W'(x) \\ H_- &= QQ^\dagger = -d^2/dx^2 + U_-(x) & U_-(x) &= W^2(x) + W'(x) \end{aligned} \quad (2.10)$$

The eigenstates ψ_k^\pm of H_+ and H_- are said to be “bosonic” and “fermionic”, respectively. In our units, we can write $H_\pm \psi_k^\pm = k_\pm^2 \psi_k^\pm$. Supersymmetry (SUSY) is said to be “spontaneously broken” if there is no bosonic zero-mode with $E_0^+ = 0$, i.e. if $\psi_0^+(x)$ is *not* normalizable. In this case, the bosonic and fermionic spectra coincide exactly,² $k_+ = k_- = k$, and the eigenstates are related by

$$\psi_k^-(x) = k^{-1} Q \psi_k^+(x), \quad \psi_k^+(x) = k^{-1} Q^\dagger \psi_k^-(x). \quad (2.11)$$

If the two couplings, g_s and g_c , of the Pöschl-Teller potential lie in the range

$$g_s \geq -\frac{1}{4}, \quad g_c \leq \frac{1}{4}, \quad (2.12)$$

¹We use units were $\hbar = \sqrt{2m} = 1$

²If the bosonic zero-mode ψ_0^+ is normalizable, i.e. if there is a state with $E_0^+ = 0$, then SUSY relates the bosonic and fermionic spectra $\{E_n^\pm\}_{n=0}^\infty$ as $E_n^- = E_{n+1}^+$.

then the two parameters defined in (2.6) are *real* and positive, $\mu \geq 0$, $\nu \geq 0$. In this case, the potential (2.1) is supersymmetric, because we can define the superpotential [27]

$$W(x) = -\alpha \left(\nu + \frac{1}{2} \right) \coth(\alpha x) + \alpha \left(\mu - \frac{1}{2} \right) \tanh(\alpha x), \quad (2.13)$$

in terms of which the Pöschl-Teller potential $\mathcal{V}(x)$ has the form (2.10), apart from a shift in the energy: $U_+(x) = \mathcal{V}(x) - \alpha^2(\mu - \nu - 1)^2$. So the Pöschl-Teller Hamiltonian can be written as the “bosonic” partner of a SUSY pair,

$$H_+^{\text{PT}} - \alpha^2(\mu - \nu - 1)^2 = Q^\dagger Q, \quad (2.14a)$$

$$H_-^{\text{PT}} - \alpha^2(\mu - \nu - 1)^2 = QQ^\dagger, \quad (2.14b)$$

with the operators Q and Q^\dagger given in (2.9) by the superpotential (2.13). In fact, the “fermionic” partner H_-^{PT} is, *again*, a Pöschl-Teller Hamiltonian. That is, the Pöschl-Teller potential is ‘*shape-invariant*’ [26]; the pair of partner potentials are

$$\begin{aligned} \mathcal{V}_+(x) &\equiv W^2(x) - W'(x) \\ &= \alpha^2 \left[\frac{\nu^2 - \frac{1}{4}}{\sinh^2(\alpha x)} + \frac{\frac{1}{4} - \mu^2}{\cosh^2(\alpha x)} + (\mu - \nu - 1)^2 \right] \\ \mathcal{V}_-(x) &\equiv W^2(x) + W'(x) \\ &= \alpha^2 \left[\frac{(\nu + 1)^2 - \frac{1}{4}}{\sinh^2(\alpha x)} + \frac{\frac{1}{4} - (\mu - 1)^2}{\cosh^2(\alpha x)} + (\mu - \nu - 1)^2 \right] \end{aligned} \quad (2.15)$$

and one can see that $\mathcal{V}_+(x)$ and $\mathcal{V}_-(x)$ “have the same shape”, i.e. they are the same function of x , only with shifted parameters. More precisely, discounting the energy shift, we have the pair of Pöschl-Teller potentials

$$\begin{aligned} \mathcal{V}(x; \mu, \nu) &\equiv \mathcal{V}_+(x) - \alpha^2(\mu - \nu - 1)^2 = \alpha^2 \left[\frac{\nu^2 - \frac{1}{4}}{\sinh^2(\alpha x)} + \frac{\frac{1}{4} - \mu^2}{\cosh^2(\alpha x)} \right] \\ \tilde{\mathcal{V}}(x; \tilde{\mu}, \tilde{\nu}) &\equiv \mathcal{V}_-(x) - \alpha^2(\mu - \nu - 1)^2 = \alpha^2 \left[\frac{\tilde{\nu}^2 - \frac{1}{4}}{\sinh^2(\alpha x)} + \frac{\frac{1}{4} - \tilde{\mu}^2}{\cosh^2(\alpha x)} \right] \end{aligned} \quad (2.16)$$

which only differ by the shifted parameters

$$\nu \mapsto \tilde{\nu} = \nu + 1, \quad \mu \mapsto \tilde{\mu} = \mu - 1. \quad (2.17)$$

SUSY and shape-invariance give us a criterion to fix the boundary condition of the eigenfunctions at the singularity in the part of the weak-medium region of coupling space where $0 < \nu < 1$ is real (yellow patch of Fig.2). If we assume that the bosonic potential $\mathcal{V}_+(x)$ is in this region, then (2.17) shows that its fermionic partner $\mathcal{V}_-(x)$ will be in the

strongly repulsive region, where \tilde{g}_s has $\tilde{\nu} > 1$ (red patch of Fig.2). In the strongly repulsive region, the zero-energy wave function is not normalizable, so SUSY is spontaneously broken, and we can relate every strongly-repulsive eigenstate $\psi_k^-(x)$, which are well-defined, to a weak-medium eigenstate $\psi_k^+(x)$, via Eqs.(2.11). Hence the well-defined functions in the red patch fix the boundary conditions of the otherwise ill-defined functions in the yellow patch.

In order to make it very clear how imposing SUSY fixes the boundary conditions in the weak-medium region, recall that, in this region, the most general solution behaves for $x \rightarrow 0$ as

$$\psi_k^+(x) \approx A_k x^{\nu+\frac{1}{2}} + B_k x^{-\nu+\frac{1}{2}}, \quad 0 < \nu < 1. \quad (2.18)$$

This function is square-integrable at $x = 0$ for any choice of A_k or B_k . From Eq.(2.11), the partner state is

$$\psi_k^-(x) = k^{-1} Q \psi_k^+(x) \approx c_1 A_k x^{\nu-1+\frac{1}{2}} + c_2 B_k x^{-\nu-1+\frac{1}{2}}, \quad 0 < \nu < 1. \quad (2.19)$$

with k -dependent constants c_1, c_2 . This latter function is only square-integrable if $B_k = 0$. So, in short, although generic functions (2.18) are always square-integrable in the weak-medium range, only the functions

$$\psi_k^+(x) \approx A_k x^{\nu+\frac{1}{2}}, \quad 0 < \nu < 1, \quad (2.20)$$

match the supersymmetric relation between the strongly-repulsive and the medium-weak regions of coupling space. Hence, to enforce the naturally existing supersymmetry of the Hamiltonians of these two regions, we must fix the (otherwise arbitrary) boundary conditions in the medium-weak region as in (2.20).

3 The renormalization group of the Pöschl-Teller potential

One way of making the boundary conditions well-defined is to perform a *renormalization* of the potential near the singularity. Renormalization of the conformal potential is well-known [17–22]; the result is technically equivalent to the construction of a self-adjoint extension of the Hamiltonian [4], but with the advantage of providing a clear physical interpretation to the parameters involved.

3.1 Renormalization

To perform the renormalization of the Pöschl-Teller potential, we adopt a general approach that does not require, *a priori*, imposing boundary conditions at the origin, nor defining an explicit regulating potential, and, most importantly, that can be used for any potential with an inverse-square singularity. The first step is to introduce an arbitrary cutoff R ,

below which we replace the singular part of $\mathcal{V}(x)$ by an arbitrary function $f(x/R)$,

$$\mathcal{V}_R(x) = \begin{cases} \mathcal{V}(x) & x > R \\ \frac{\lambda(R)}{R^2} f(x/R) & 0 < x < R \end{cases} \quad (3.1)$$

We only require that $f(x)$ is not singular at $x = 0$. The parameter $\lambda(R)$ (which does not depend on x) is introduced so that $f(1) = 1$. Usually, f is chosen to be a step function [20], but it is not necessary to specify it at all. The regularization procedure can be thought of in terms of an ‘effective’ description of the singularity, see e.g. [18]. We look for solutions outside the “core region” $x < R$, and assume that, at energies k that are small compared with the energy scale $1/R$, i.e. for

$$kR \ll 1, \quad (3.2)$$

physics must be insensitive to what happens inside in the regularized core.

Let us denote the “unphysical” wave function inside the regularized region $x < R$ by $\psi_k^<(x)$. Eq.(2.2) reads

$$\frac{d^2\psi_k^<(x)}{dx^2} + \left(\frac{(kR)^2 - \lambda(R)f(x/R)}{R^2} \right) \psi_k^<(x) = 0. \quad (3.3)$$

At energies for which the effective description is valid, $kR \ll 1$, we can neglect the term $(kR)^2$, and Eq.(3.3) becomes independent of k . The solution $\psi_k^<$ for $k \neq 0$ is then the same as the solution $\psi_0^<$ for $k = 0$. By continuity, so are their logarithmic derivatives,

$$\psi_k'^<(R)/\psi_k^<(R) = \psi_0'^<(R)/\psi_0^<(R) \equiv \mathcal{F}(R), \quad (3.4)$$

where $\mathcal{F}(R)$, by definition, does not depend on k . The wave function and its first derivative must be continuous for all x , so we conclude that

$$\mathcal{F}(R) = \frac{\psi_0'(R)}{\psi_0(R)}, \quad (3.5)$$

where $\psi_0(x)$ is the “physical” solution *outside* the regularized region, and, more generally,

$$\frac{\psi_k'(R)}{\psi_k(R)} = \mathcal{F}(R) \quad \text{for} \quad kR \ll 1. \quad (3.6)$$

So the renormalization procedure amounts to imposing Robin boundary conditions at the regulating point $x = R$, without specifying any conditions at the singular point $x = 0$.

It is important to emphasize that the function $\mathcal{F}(R)$ is *defined* by Eq.(3.4), hence it is completely (although indirectly) fixed by the “strength” of the potential inside the regularizing core,³ i.e. by $\lambda(R)f(x/R)$, through the logarithmic derivative of the function

³This point of view, of making the amplitude of the regularizing potential change with R , is analogous to the “core renormalization framework” of [18].

$\psi_0^<(x)$. That is to say, $\mathcal{F}(R)$ does not depend in any way on what happens outside the regularizing core. In particular, it does not depend on the form of the pair of independent solutions of the Pöschl-Teller Schrödinger equation (2.2). The meaning of Eq.(3.6) is that, for a given value of R , the number $\mathcal{F}(R)$ — which is independent of the Schrödinger equation — *fixes the boundary conditions* of the otherwise general solution (2.4) of Eq.(2.2). In other words, $\mathcal{F}(R)$ defines a relation between the integration constants A_k and B_k .

We can find this relation as follows. First, it is convenient to define the dimensionless quantity

$$\gamma(R) \equiv -\frac{1}{2} + R\mathcal{F}(R), \quad (3.7)$$

and work with $\gamma(R)$ instead of $\mathcal{F}(R)$. Now, note that we can always compute $\mathcal{F}(R)$, and hence $\gamma(R)$, from the zero-energy solution of the Pöschl-Teller potential, since when $k = 0$ condition (3.2) is identically satisfied. The result for $\gamma(R)$ can be organized as a ratio of two series in powers of (αR) , see Appendix A. Since $1/\alpha$ is the characteristic length scale of the Pöschl-Teller potential, we must take

$$\alpha R \ll 1. \quad (3.8)$$

(Otherwise the potential would become too disfigured by a large regularized region.) Thus we find

$$\gamma(R) = \nu \frac{1 - \varepsilon(L/R)^{2\nu}}{1 + \varepsilon(L/R)^{2\nu}} \quad (3.9)$$

ignoring terms of order αR . Here

$$\varepsilon \equiv \text{Sign}[B_0/A_0] = \pm 1, \quad (3.10)$$

and we have defined

$$L^{2\nu} \equiv |B_0/A_0|, \quad (3.11)$$

which is an intrinsic and *arbitrary* length scale contained in the solution $\psi_0(x)$ given by Eq.(2.4). We are assuming for now that $\nu > 0$ is real. If we compute the equivalent of the r.h.s. of Eq.(3.7), in the effective regime (3.2), and taking (3.8) and (3.6) into account, the result must coincide with the r.h.s. of Eq.(3.9). (See Eq.(A.5) in Appendix A.) As a consequence,

$$B_k/A_k = \varepsilon L^{2\nu}, \quad (3.12)$$

which holds for all k when we take $R \rightarrow 0$. In other words, the ratio of the integration constants B_k/A_k does not depend on k .

3.2 Breaking of asymptotic conformal symmetry

We can associate a renormalization group (RG) flow to the renormalization above. We interpret $\gamma(R)$ as a ‘running coupling’.⁴ (In fact, the specific form of Eq.(3.7) is in fact

⁴NB: When we refer to ‘coupling space’, we always mean only the couplings g_s , g_c of the Pöschl-Teller potential.

inspired by the RG of the conformal potential, see e.g. [22, 24, 25].) The flow of $\gamma(R)$ is characterized by its beta function

$$\beta(\gamma) \equiv \frac{d\gamma}{d \log R}. \quad (3.13)$$

Now, note that, if we take the derivative of $\gamma(x) = -\frac{1}{2} + x\psi'_0(x)/\psi_0(x)$, use the Schrödinger equation, then evaluate the result at $x = R$, we find

$$\beta(\gamma) = -\gamma^2 + \frac{1}{4} + R^2 \mathcal{V}(R). \quad (3.14)$$

Expanding $\mathcal{V}(x)$ up to first order in x , Eq.(3.14) gives

$$\beta(\gamma) = -(\gamma + \nu)(\gamma - \nu) - \frac{1}{3}(\nu^2 + 3\mu^2 - 1)(\alpha R)^2 + \mathcal{O}(\alpha R)^4 \quad (3.15)$$

Here it is understood that we must find $R = R(\gamma)$, to eliminate R from the r.h.s. in favor of γ , by inverting Eq.(A.1). As shown in Appendix A, this is difficult to do analytically, even at lowest order, because of the terms $(L/R)^{2\nu}$ in the asymptotic expansion of $\gamma(R)$.

3.2.1 Spontaneous and explicit symmetry breaking

Near the singularity, if we make $\alpha R \rightarrow 0$ in Eq.(3.15), we find

$$\beta(\gamma) = -(\gamma + \nu)(\gamma - \nu) + \dots \quad (3.16)$$

which is consistent with $\gamma(R)$ given by Eq.(3.9). The dots indicate terms that we have neglected when taking $\alpha R = 0$. Eq.(3.16) is the beta-function of the conformal potential [19], as expected, since we are in the asymptotic region where the Pöschl-Teller becomes conformal. The RG flow driven by (3.16) has two fixed points, where $\beta(\gamma) = 0$,

$$\gamma_{\text{IR}} = +\nu, \quad \gamma_{\text{UV}} = -\nu. \quad (3.17)$$

We will call them “fixed points”, but with the understanding that (3.16) is *not*, of course, the exact beta-function for the Pöschl-Teller potential. The point $\gamma = +\nu$ is an IR fixed point, in the sense that it is reached at “long distances”,

$$R/L \gg 1; \quad (3.18)$$

while $\gamma = -\nu$ is a UV fixed point, reached at “small distances”,

$$R/L \ll 1. \quad (3.19)$$

Thus L causes a *spontaneous breaking* of the “classical” asymptotic conformal symmetry of the Pöschl-Teller potential. The same phenomenon is found in the exact conformal potential [19, 22, 24, 25]. But, while the inverse-square potential has no intrinsic length scale,

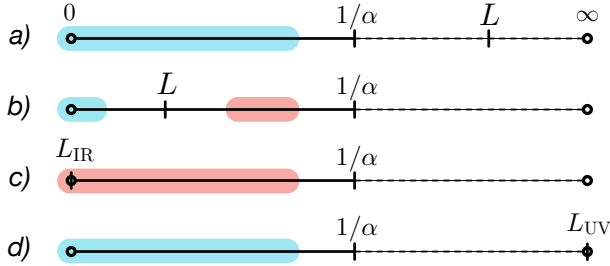


Figure 3: Ranges of the cutoff R , depending on the position of the anomalous scale L . Red indicates a IR regime (3.18), and blue a UV regime (3.19).

the Pöschl-Teller potential has $1/\alpha$, which causes an *explicit breaking* of the asymptotic conformal symmetry.

We have a hierarchy of scales: depending on whether $\alpha L \leq 1$, conformal symmetry may be broken either spontaneously or explicitly first. We can look at the limits (3.18) and (3.19) in units of $1/\alpha$, as $\alpha R/\alpha L$. If $\alpha L \geq 1$, then we are of course forced to stay inside the UV region, as in Fig.3a, and the symmetry is explicitly broken before L plays its part. But if L is a “quantum” scale, in the sense that $\alpha L \ll 1$, we can slide the cutoff from the UV deep into the IR region, while keeping $\alpha R \ll 1$, as in Fig.3b, so L spontaneously breaks the asymptotic symmetry before $1/\alpha$ does. More precisely, in this latter case, the nature of the asymptotic RG flow depends on the sign $\varepsilon = \pm 1$. Looking at $\gamma(R)$ in Eq.(3.9), we see a “massless RG flow” for $\varepsilon = +1$, with the scale R/L free to run across the UV and IR fixed regions. If $\varepsilon = -1$, on the other hand, L behaves like a “QCD scale”, where the coupling $\gamma(R)$ diverges, and the flow ends in a massive phase with mass scale $1/L$.

In any case, we emphasize that *if L is finite, it is always impossible to actually reach the IR fixed point*, since this requires that $R \rightarrow \infty$ in (3.9). Thus the RG flow always has a massive phase, with mass scale given by α . What may happen is that, if αL is very small, but not zero, the asymptotic beta function (3.16) will hold for a long while as $\gamma(R)$ leaves the UV fixed point $\gamma_{\text{UV}} = -\nu$; then, as $\gamma(R) \rightarrow +\nu$, the running coupling may start to “walk”. But eventually the αR corrections become relevant, and the flow becomes massive. Finding the effect of α and its explicit symmetry breaking in the beta function is complicated because it requires inverting a series for $\gamma(R)$ and, if L is finite, this series has a complicated structure, as discussed in Appendix A, see Eq.(A.1).

3.2.2 RG flows without spontaneous symmetry breaking

There are two possible ways of getting rid of the anomalous dimension: by taking

$$L_{\text{IR}} = 0 \quad \text{or} \quad L_{\text{UV}} = \infty. \quad (3.20)$$

If we fix $L = L_{\text{IR}}$, the IR regime (3.19) extends to all values of R , as in Fig.3c. Fixing $L = L_{\text{UV}}$ instead, it is the UV regime (3.18) that extends to all values of R , as in Fig.3d. In both cases, the conformal coupling (3.9) stops running; for $L = \infty$, it stays fixed at the UV fixed point $\gamma_{\text{UV}} = -\nu$, and, for $L = 0$, it stays at the IR fixed point $\gamma_{\text{IR}} = \nu$. Note that this latter case is the only way of actually reaching the IR fixed point of the conformal beta function (3.16). This is an important fact: the IR fixed point $\gamma_{\text{IR}} = \nu$ only becomes accessible if $L = 0$ *exactly*; otherwise, it is always hidden above the scale $1/\alpha$.

This “discontinuity” — the fact that $\gamma_{\text{IR}} = \nu$ is only accessible “non-perturbatively” (in the value of L) — is associated with a drastic change in the RG flow when L is set to one of the points (3.20). Conformal symmetry is now necessarily broken explicitly, by the scale $1/\alpha$, since there is no anomalous scale to break it spontaneously. To find the beta function, we must take αR terms into account in computing the running coupling $\gamma(R)$, hence we cannot use neither (3.9) nor (3.16), which discarded αR terms completely. We have to compute both $\gamma(R)$ and $\beta(\gamma)$ from the start, in each case (3.20). Fortunately, here it *is* possible to compute perturbatively both functions, as the structure of the αR series completely changes when we eliminate L , as discussed in Appendix A.

In fact, we find two *distinct* RG flows, one going out of each point $\gamma = \pm\nu$. Note that, the conformal beta function (3.16) is not a function anymore, but instead a “beta constant”, $\beta(\pm\nu) = 0$. It ceases to be constant only when we find the α corrections. Computing $\gamma(R)$ from $\psi_0(x)$, using (3.11) to fix the constants A_k, B_k , we find, at leading order,

$$\text{for } L = L_{\text{IR}}: \quad \gamma(R) = +\nu - \frac{\nu^2 + 3\mu^2 - 1}{6(1 + \nu)}(\alpha R)^2 + \dots \quad (3.21)$$

$$\text{for } L = L_{\text{UV}}: \quad \gamma(R) = -\nu - \frac{\nu^2 + 3\mu^2 - 1}{6(1 - \nu)}(\alpha R)^2 + \dots \quad (3.22)$$

These show how $\gamma(R)$ leaves the “previously fixed points” $\gamma = \pm\nu$. In each case we have a *different* beta function, that can be expanded perturbatively near the respective points as

$$\beta_{\text{IR}}(\gamma) = 2(\gamma - \nu) + \dots \quad (3.23)$$

$$\beta_{\text{UV}}(\gamma) = 2(\gamma + \nu) + \dots \quad (3.24)$$

Note that these functions are *not* given by the limits of (3.16) for $\gamma \rightarrow \pm\nu$. In particular, while in (3.16) the point $\gamma = +\nu$ was a IR stable fixed point (i.e. with decreasing $\beta(\gamma)$), here *both* beta functions are UV stable (both are *increasing*). This is expected: for finite L , one goes toward the point $\gamma = +\nu$ at *large* R but, despite the IR/UV nomenclature associated with the value of L , in Eqs.(3.21)-(3.22) we now arrive at *both* fixed points $\gamma = \pm\nu$ by taking a *small* distance cutoff R . So both cases are UV limits.

Choosing $L = L_{\text{IR}}$ or L_{UV} corresponds to choosing one of the (sets of) integration constants A_k or B_k to vanish; in the IR, $B_k = 0$, and, in the UV, $A_k = 0$. In the strongly

repulsive region of parameter space, normalizability of $\psi_k(x)$ enforces $L = L_{\text{IR}}$, recovering the asymptotic conformal symmetry. Similarly, the discussion of Sect.2.2 shows that *we can use SUSY to reestablish the asymptotic conformal symmetry* in part of the weak-medium region where the Pöschl-Teller potential is supersymmetric, by setting $L = L_{\text{IR}}$.

3.2.3 The critical line $\nu = 0$

The two fixed points $\gamma = \pm\nu$ merge if $\nu = 0$. The critical line in the g_c - g_s plane where this happens is precisely the line $g_s = -\frac{1}{4}$, which marks the boundary between the medium-weak and strongly attractive regions, cf. Fig.2. On this critical line, solution (2.4) is not valid; the correct solution of the Schrödinger equation is the one given in Eq.(B.2) in Appendix B. Because of this, we cannot simply take the limit $\nu \rightarrow 0$ in the formulas for the RG flow derived above, since they were all deduced from the solution (2.4).

The details of the renormalization and the computation of the running coupling in this case are given in Appendix B. Using the asymptotic solution (B.3) with $k = 0$, we can compute the running coupling

$$\gamma(R) = -\frac{\mathcal{D}}{1 - \mathcal{D} \log(\alpha R)} \quad (3.25)$$

where \mathcal{D} is a *dimensionless* constant, that plays a paper similar to L , cf. Eq.(B.7). Interestingly, now αR appears logarithmically in $\gamma(R)$. The presence of the logarithmic branch in Eq.(2.3) is precisely why this solution must be considered separately. The beta function $\beta = d\gamma/d \log R$ reads

$$\beta(\gamma) = -\gamma^2 + \dots \quad (3.26)$$

which agrees with Eq.(3.16) in the limit $\nu \rightarrow 0$. The UV and IR fixed points of the conformal beta function, $\gamma = \pm\nu$, here coalesce into one *marginal* fixed point $\gamma = 0$. This is a kind of Berezinskii-Kosterlitz-Thouless (BKT) phase transition [28, 29].

The dots in Eq.(3.26) hide terms that are perturbative in αR , as in (3.16). But because there is also a logarithmic contribution of αR , here we cannot separate the effects of “spontaneous versus explicit” breaking of conformal symmetry, as done above. Instead, the scale $1/\alpha$ appears along with the parameter \mathcal{D} , which is related to the ratio of integration constants of the solution (B.2). So, even without taking the αR corrections into account, we see that, as R increases, the running coupling (3.25) diverges in a massive RG flow with mass scale

$$1/L_0 = \alpha e^{-1/\mathcal{D}}. \quad (3.27)$$

We could suppress this massive phase by suppressing the logarithmic solution near the origin, which amounts to choosing the corresponding integration constants of the Schrödinger equation as $\mathcal{B}_k = 0$, which makes $\mathcal{D} = 0$; cf. Eq.(B.8). Then we would need to compute the perturbative powers of αR in (3.26) to find the (explicit) breaking of conformal symmetry.

3.2.4 Strongly attractive coupling and the phase θ

For the strongly attractive regime, where $g_s < -\frac{1}{4}$, and $\nu = i|\nu|$, instead of the anomalous length scale L , renormalization introduces a *phase* θ . Here, the constants A_k and B_k are complex, and conjugates of one another, cf. Eq.(2.7b). For $k > 0$, we can parameterize them in a convenient polar form in terms of real functions C_k and $\zeta(k)$,

$$A_k = \frac{k^{i|\nu|}}{2i} C_k e^{i\zeta(k)} = B_k^*. \quad (3.28)$$

For $k = 0$ this parametrization is ill defined, and instead we choose

$$A_0 = \frac{\alpha^{i|\nu|}}{2i} C_0 e^{i\theta} = B_0^*. \quad (3.29)$$

Then the asymptotic behavior (2.7b) reads

$$\psi_k(x) \approx C_k x^{\frac{1}{2}} \sin [|\nu| \log(kx) + \zeta(k)] \quad (3.30a)$$

$$\psi_0(x) \approx C_0 x^{\frac{1}{2}} \sin [|\nu| \log(\alpha x) + \theta]. \quad (3.30b)$$

The function $\mathcal{F}(R)$ can be computed from Eq.(3.6) using $\psi_0(x)$ and $\psi_k(x)$. The renormalization framework identifies the two results, yielding

$$(k/\alpha)^{2i|\nu|} e^{2i\zeta(k)} = e^{i\theta}, \quad 0 \leq \theta < 2\pi \quad (3.31)$$

which can also be written as $|\nu| \log(k/\alpha) + \zeta(k) = \theta - n\pi$, with $n \in \mathbb{N}$. For bound states, this equation discretizes the wave vector k . If the potential were exactly the conformal potential, then ζ would be independent of k , and we would have $k_n = k_0 e^{-n\pi/|\nu|}$ [17, 20, 21]. For the Pöschl-Teller potential, the phase $\zeta(k)$ is determined in terms of the arbitrary renormalization parameter θ , and fixed by the other boundary condition at $x \rightarrow \infty$; see §4.1.2.

Computing $\mathcal{F}(R) = \psi'_0(x)/\psi_0(x)$ from the asymptotic solution (3.30b), we find the running coupling (3.7) to be

$$\gamma(R) = |\nu| \cot [|\nu| \log(\alpha R) + \theta]. \quad (3.32)$$

Again, we have a logarithmic contribution from αR , as in the $\nu = 0$ case. Again, this stems from a logarithmic branch in the solution (3.30). The corresponding asymptotic beta function is, again, as in Eq.(3.16), but with $\nu = i|\nu|$,

$$\beta(\gamma) = -\gamma^2 - |\nu|^2 + \dots \quad (3.33)$$

Now there are no fixed points, not even at $R = 0$. The two points $\gamma = \pm\nu$, which merged in the BKT phase transition when $\nu = 0$, now have completely disappeared, and conformal symmetry is necessarily broken. The RG flow is massive, with every value of $\gamma(R)$ reached for a *finite* range of R . There are two ends of the massive flow, with mass scales $\alpha e^{\theta/|\nu|}$ and $\alpha e^{(\theta-\pi)/|\nu|}$. As in the $\nu = 0$ case, we cannot separate the effects of the explicit and the spontaneous breaking of conformal symmetry, because α necessarily appears in the mass scales of the RG flow together with θ , even if we neglect perturbative corrections to (3.33).

4 Spectra of the Pöschl-Teller Hamiltonian

The presence of the scale L or the phase θ influences the spectrum of the Pöschl-Teller Hamiltonian. For example, it can be expected that, as it breaks the asymptotic conformal symmetry, L may produce a bound state confined to the region very near the singularity. Every aspect of the spectrum can be read from the S-matrix

$$S \equiv e^{2i\delta(k)}, \quad (4.1)$$

defined by the phase shift $\delta(k)$, such that the asymptotic solution for $kx \gg 1$ is

$$\begin{aligned} \psi_k(x) &\sim e^{i\delta(k)} \sin [k(x - \Delta x) + \delta(k)] \\ &= \sin [k(x - \Delta x)] + e^{i\delta(k)} e^{ik(x - \Delta x)} \sin \delta(k). \end{aligned} \quad (4.2)$$

We will now compute the S-matrix for the Pöschl-Teller potential for any value of the renormalization scale L , including the UV and IR fixed points (3.20) of the asymptotic RG flow. As it was to be expected, the spectrum depends sensibly on the region of coupling space, besides the value of L or θ .

To do so, we expand the hypergeometric functions in (2.4) for $kx \gg 1$ (cf. e.g. [30, §15]),

$$\begin{aligned} \psi_k(x) &\approx \\ &\left[\frac{A_k}{\alpha^{\frac{1}{2}+\nu}} \frac{\Gamma(1+\nu)\Gamma(-ik/\alpha)}{\Gamma(\frac{1+\nu+\mu-ik/\alpha}{2})\Gamma(\frac{1+\nu-\mu-ik/\alpha}{2})} + \frac{B_k}{\alpha^{\frac{1}{2}-\nu}} \frac{\Gamma(1-\nu)\Gamma(-ik/\alpha)}{\Gamma(\frac{1-\nu+\mu-ik/\alpha}{2})\Gamma(\frac{1-\nu-\mu-ik/\alpha}{2})} \right] \frac{e^{-ikx}}{2^{-\frac{ik}{\alpha}}} \\ &+ \left[\frac{A_k}{\alpha^{\frac{1}{2}+\nu}} \frac{\Gamma(1+\nu)\Gamma(ik/\alpha)}{\Gamma(\frac{1+\nu+\mu+ik/\alpha}{2})\Gamma(\frac{1+\nu-\mu+ik/\alpha}{2})} + \frac{B_k}{\alpha^{\frac{1}{2}-\nu}} \frac{\Gamma(1-\nu)\Gamma(ik/\alpha)}{\Gamma(\frac{1-\nu+\mu+ik/\alpha}{2})\Gamma(\frac{1-\nu-\mu+ik/\alpha}{2})} \right] \frac{e^{ikx}}{2^{\frac{ik}{\alpha}}}. \end{aligned} \quad (4.3)$$

In the medium-weak and in the strongly repulsive regime, we can phrase the boundary conditions in the language of the RG flow to rewrite S in terms of the renormalization scale L . Comparison of (4.2) and (4.3) shows that $\Delta x \equiv \alpha^{-1} \log 2$, and the S-matrix is

$$\begin{aligned} S_L^\varepsilon(k) &= e^{2i\bar{\delta}} \left[\frac{\Gamma(1+\nu)}{\Gamma(\frac{1+\nu+\mu+ik/\alpha}{2})\Gamma(\frac{1+\nu-\mu+ik/\alpha}{2})} + \varepsilon(\alpha L)^{2\nu} \frac{\Gamma(1-\nu)}{\Gamma(\frac{1-\nu+\mu+ik/\alpha}{2})\Gamma(\frac{1-\nu-\mu+ik/\alpha}{2})} \right] \\ &\times \left[\frac{\Gamma(1+\nu)}{\Gamma(\frac{1+\nu+\mu-ik/\alpha}{2})\Gamma(\frac{1+\nu-\mu-ik/\alpha}{2})} + \varepsilon(\alpha L)^{2\nu} \frac{\Gamma(1-\nu)}{\Gamma(\frac{1-\nu+\mu-ik/\alpha}{2})\Gamma(\frac{1-\nu-\mu-ik/\alpha}{2})} \right]^{-1}, \end{aligned} \quad (4.4)$$

where

$$\exp 2i\bar{\delta} \equiv -\frac{\Gamma(ik/\alpha)}{\Gamma(-ik/\alpha)}. \quad (4.5)$$

This phase $\bar{\delta}$, which does not depend on the parameters μ, ν is a universal feature of the S-matrix of potentials that behave as $\mathcal{V}(x) \sim e^{-\alpha x}$ for $x \rightarrow \infty$. Although it contributes

to the phase shift $\delta(k)$, it will not contribute to the analysis of the spectrum to be done below. Since L is independent of k , Eq.(4.4) gives the explicit dependence of the S-matrix on the wave number k . It is the general expression, which reduces to special cases when we choose specific boundary conditions, i.e. choose L . The S-matrix simplifies considerably if we stay at one of the fixed points of RG flow. If the potential is strongly attractive, then $\nu = i|\nu|$ is complex, and instead of L we must use the phase θ defined in Eq.(3.31). In this case, we find

$$S_\theta(k) = e^{2i\bar{\delta}} \left[\frac{\Gamma(1+i|\nu|)}{\Gamma(\frac{1+i|\nu|+\mu+ik/\alpha}{2})\Gamma(\frac{1+i|\nu|-\mu+ik/\alpha}{2})} - \frac{e^{-i\theta} \Gamma(1-i|\nu|)}{\Gamma(\frac{1-i|\nu|+\mu+ik/\alpha}{2})\Gamma(\frac{1-i|\nu|-\mu+ik/\alpha}{2})} \right]^{-1} \times \left[\frac{\Gamma(1+i|\nu|)}{\Gamma(\frac{1+i|\nu|+\mu-ik/\alpha}{2})\Gamma(\frac{1+i|\nu|-\mu-ik/\alpha}{2})} - \frac{e^{-i\theta} \Gamma(1-i|\nu|)}{\Gamma(\frac{1-i|\nu|+\mu-ik/\alpha}{2})\Gamma(\frac{1-i|\nu|-\mu-ik/\alpha}{2})} \right]^{-1}. \quad (4.6)$$

Again, we have an explicit expression for how the S-matrix depends on k , for all possible choices of boundary conditions parameterized by θ .

The S-matrices above describe scattering off the Pöschl-Teller potential in each regime of its couplings. The potential always has a continuous spectrum for $E > 0$, that is, for real $k > 0$, since $\mathcal{V}(x) \rightarrow 0$ for large x . For the continuum of states, the phase shift $\delta(k) = \frac{1}{2i} \log S(k)$ is a real number, as can be seen most easily from the first equality in (4.2), given that $\psi_k(x)$ is real. Meanwhile, for some ranges of g_s and g_c , the potential also develops metastable, bound or anti-bound states; these can also be discovered by looking at the analytic properties of the S-matrices.

Bound states have negative energy, $E = \hbar^2 k^2 / 2m < 0$, hence

$$k = i\kappa, \quad \kappa > 0, \quad (4.7)$$

is imaginary. By definition the wave-function vanishes at infinity, which means that the first, divergent term $\sim e^{-ikx}$ in the r.h.s. of Eq.(4.3), must be set to zero. This amounts to setting to zero the square brackets that appear in the denominator of the S-matrix (4.4), that is, bound states are poles of $S(\kappa)$, excepted the poles of $e^{2i\bar{\delta}}$.

We can also have different kinds of ‘metastable’ states. These are solutions whose stationary part behave, again, as an outgoing wave at infinity, $\psi(x) \sim e^{ikx}$, hence they are, again, poles of the S-matrix. But now we allow the wave number to have an imaginary part,

$$k = k_r - i\kappa, \quad \begin{cases} k_r > 0 \\ \kappa \in \mathbb{R} \end{cases} \quad (4.8)$$

Although the stationary part of the wave-function, $\psi_k(x) \sim e^{ikx}$, is not square-integrable anymore, the time-dependence of the total function is given by

$$\exp\left(-\frac{iEt}{\hbar}\right) = \exp\left(-\frac{i\hbar(k_r^2 - \kappa^2)t}{2m}\right) \exp\left(-\frac{\hbar k_r \kappa}{m}t\right). \quad (4.9)$$

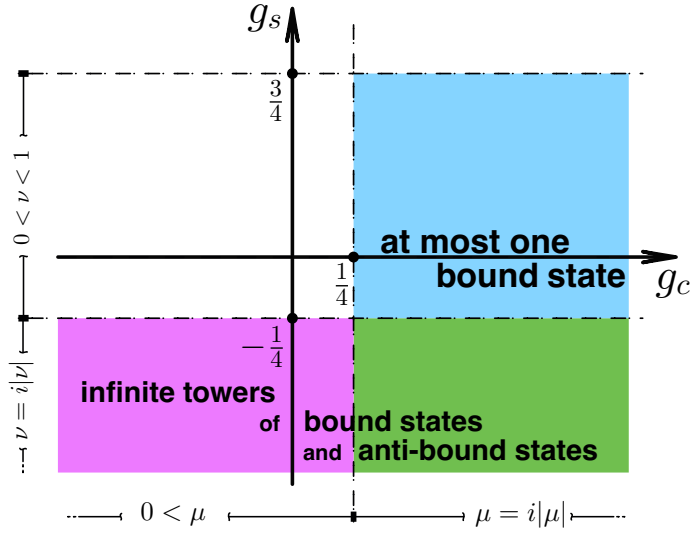


Figure 4: Regions in parameter space where the IR boundary condition cannot be fixed. We indicate the spectra outside of the two fixed points, where the length scale L or the phase θ are finite.

So, if $\kappa > 0$, the wave function decays exponentially with time, and the state is metastable, with a lifetime

$$\tau = \frac{2m}{\hbar k_r \kappa}. \quad (4.10)$$

If κ is small, this metastable state has a large lifetime, producing a peak in the scattering cross-section, so it is a ‘resonance’. Still for $\kappa > 0$, if there are poles with $k_r = 0$, these are called ‘anti-bound states’. Again, these states are not normalizable (since $\psi \sim e^{\kappa x}$ diverges), but the real exponential in (4.9) suppresses the total wave function, and the states have a discrete energy spectrum.

If there are poles of the S-matrix with $\kappa < 0$ and $k_r \neq 0$, the real exponential in (4.9) diverges and the system is unstable.

4.1 Spectrum at arbitrary L or θ

In the regions of parameter space shown in Fig.4, we have no reason for fixing the the renormalization scale L or the phase θ to any specific value. The search for poles can be divided into the blue region, where we have the scale L , and the purple and green regions, where we have the phase θ .

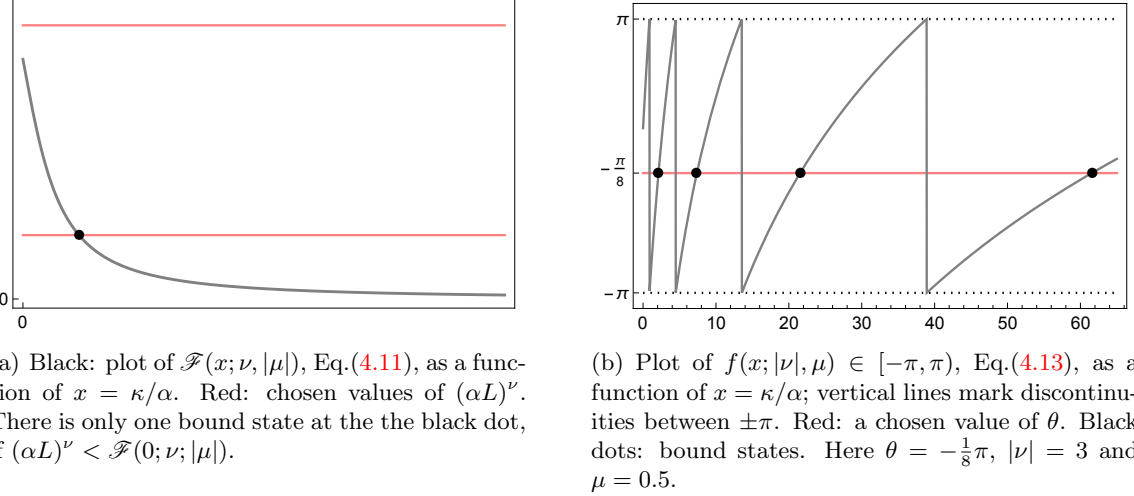


Figure 5

4.1.1 The medium-weak region

In the blue patch of parameter space shown in Fig.4, the potential is in the medium-weak range but is *not* supersymmetric, then we cannot use SUSY to fix $L = 0$. The absence of SUSY is due to $g_c > \frac{1}{4}$, which makes μ purely imaginary, so we can set $\mu = i|\mu|$; note also that $0 < \nu < 1$.

Let us first search for bound states, with $k = i\kappa$, and $\kappa > 0$. Inspection of (4.4) shows that at poles of $S_L^\pm(k)$ the dividing square bracket must have a simple zero,

$$-\varepsilon(\alpha L)^{2\nu} = \frac{\Gamma(1 + \nu)}{\Gamma(1 - \nu)} \frac{\Gamma(\frac{1-\nu+i|\mu|+\kappa/\alpha}{2})\Gamma(\frac{1-\nu-i|\mu|+\kappa/\alpha}{2})}{\Gamma(\frac{1+\nu+i|\mu|+\kappa/\alpha}{2})\Gamma(\frac{1+\nu-i|\mu|+\kappa/\alpha}{2})} \equiv \mathcal{F}(\kappa/\alpha; \nu, |\mu|). \quad (4.11)$$

The function $\mathcal{F}(\kappa/\alpha; \nu, |\mu|)$ thus defined is *real*, even though there are Gamma functions with complex arguments in the second fraction, because the latter appear in products of the type $\Gamma(z)\Gamma(\bar{z}) = |\Gamma(z)|^2$. Hence the second fraction in (4.11) is never negative; neither is the first fraction, because $0 < \nu < 1$, and we conclude that $\mathcal{F} \geq 0$.

We can thus conclude that Eq.(4.11) does not have a solution if the l.h.s. is negative, that is $S_L^+(\kappa)$ has no poles, and *there are no bound states* in this case.

If the r.h.s. of Eq.(4.11) is positive, we may have solutions. In Fig.5(a) we plot the typical behavior of \mathcal{F} as a function of $\kappa/\alpha \geq 0$. It is a decreasing, monotonic function, which goes to zero at infinity, and has its largest value at $\kappa = 0$. As a consequence, Eq.(4.11) has only one solution if

$$0 < (\alpha L)^{2\nu} < \mathcal{F}(0; \nu; |\mu|), \quad (4.12)$$

and no solution if $(\alpha L)^{2\nu} > \mathcal{F}(0; \nu; |\mu|)$. In short, $S_L^-(\kappa)$ can have at most one pole, hence *at most one bound state, depending on the scale parameter L* .

Inspection of the S-matrix (4.4) for $k = k_r - i\kappa$, with $\kappa > 0$, shows that *there are no metastable nor anti-bound states for arbitrary L* . But we do find them for $L = \infty$, i.e. at the UV fixed point, as we show in Sect.4.3 below.

4.1.2 The strongly attractive region

In the strongly attractive region $g_s < -\frac{1}{4}$, the S-matrix is given by Eq.(4.6), in terms of the arbitrary phase θ . Now $\nu = i|\nu|$ is an imaginary number in the positive imaginary axis. We are in the green and purple regions of Fig.4.

Let us first search for bound states. Set $k = i\kappa$, with $\kappa > 0$. Once more, we search for zeros of the whole denominator of (4.6), i.e. solution of

$$e^{i\theta} = \frac{\Gamma(1 - i|\nu|)}{\Gamma(1 + i|\nu|)} \frac{\Gamma(\frac{1+i|\nu|+\mu+\kappa/\alpha}{2})\Gamma(\frac{1+i|\nu|-\mu+\kappa/\alpha}{2})}{\Gamma(\frac{1-i|\nu|+\mu+\kappa/\alpha}{2})\Gamma(\frac{1-i|\nu|-\mu+\kappa/\alpha}{2})} \equiv \exp if(\kappa/\alpha; |\nu|, \mu). \quad (4.13)$$

By fixing the relation between θ and k , this equation also fixes the phase $\zeta(k)$ in Eq.(3.31) and completes the description of the eigenstates.

The bound states are those κ which solve Eq.(4.13), i.e. for which $\theta = f(\kappa/\alpha; |\nu|, \mu)$. The analysis of this equation is more conveniently done graphically. In Fig.5(b) we plot $f(x; |\nu|, \mu)$ as a function of $x = \kappa/\alpha$, for representative values of $|\nu|$ and μ . We see that there is an infinite number of bound states given by the solutions κ_n . There is no defined value for the lowest energy, i.e. no maximum value of κ_n . Moreover, the lower the energy $E_n \sim -\kappa_n^2$, the larger is the gap $\Delta E_{n,n+1}$ between consecutive bound states. The numerical values of the first five solutions κ_n of Eq.(4.13), for the parameters in $|\nu| = 3$, $\mu = 0.5$ used in the example of Fig.5(b), are

$$\frac{\kappa_1}{\alpha} = 2.1178, \quad \frac{\kappa_2}{\alpha} = 7.3824, \quad \frac{\kappa_3}{\alpha} = 21.5399, \quad \frac{\kappa_4}{\alpha} = 61.5593, \quad \frac{\kappa_5}{\alpha} = 175.4851.$$

The ratios between consecutive levels,

$$\frac{\kappa_2}{\kappa_1} = 3.4859, \quad \frac{\kappa_3}{\kappa_2} = 2.9177, \quad \frac{\kappa_4}{\kappa_3} = 2.85792, \quad \frac{\kappa_5}{\kappa_4} = 2.85067,$$

approach the value $e^{\pi/|\nu|} \approx 2.8497$ for $|\nu| = 3$. That is, as we increase n ,

$$\kappa_{n+1}/\kappa_n \approx e^{\pi/|\nu|}, \quad n \gg 1. \quad (4.14)$$

Recall that here we are in the strongly attractive regime; the bound states are essentially locked inside the pit near the origin, where $\mathcal{V} \approx g_s/x^2$. This is why the behavior of bound states that we find here is similar to the Efimov effect for the conformal potential [31]. However, here the bound states do not accumulate near the threshold of zero energy: for

small κ the wave functions with $E \approx 0$ spread farther from the origin, and feel the difference between the Pöschl-Teller and the conformal potentials. The example above corresponds to a point with $\mu > 0$ (purple region in Fig.4), but the results are analogous for imaginary μ (green region in Fig.4).

We now search for metastable states. For a given (real) θ , the poles of the S-matrix (4.6) with $k = k_r - i\kappa$ are the solutions of

$$e^{i\theta} = \frac{\Gamma(1 - i|\nu|)}{\Gamma(1 + i|\nu|)} \frac{\Gamma(\frac{1+i|\nu|+\mu}{2} - \frac{\kappa+ik_r}{2\alpha})\Gamma(\frac{1+i|\nu|-\mu}{2} - \frac{\kappa+ik_r}{2\alpha})}{\Gamma(\frac{1-i|\nu|+\mu}{2} - \frac{\kappa+ik_r}{2\alpha})\Gamma(\frac{1-i|\nu|-\mu}{2} - \frac{\kappa+ik_r}{2\alpha})} \equiv \exp i\bar{f}(\kappa/\alpha; |\nu|, \mu). \quad (4.15)$$

For the equation to have a solution, we must have $\bar{f} \in \mathbb{R}$, which means that the combination of Gamma functions must be a phase, i.e. its modulus squared must be one. This holds if and only if $k_r = 0$; in this case, the every Gamma function in the numerator of (4.15) is the complex conjugate of the corresponding Gamma function in the denominator below, hence the square modulus of the expression is one. If $k_r \neq 0$, this matching of complex conjugate numbers is spoiled. Since k_r is forced to vanish, *there are no metastable states in the strongly attractive region*.

Setting $k_r = 0$, we find *an infinite series of anti-bound states*, with $\kappa > 0$. Again, this is best seen graphically, and shown in Fig.6(a). We plot $\bar{f}(\kappa/\alpha; |\nu|, \mu) \in [-\pi, +\pi]$. The anti-bound states are at the intersections with a horizontal line that marks a chosen value of θ . In our example, we chose $|\nu| = 3.00$, $\mu = 1.72$ and $\theta = -\frac{\pi}{10}$; in this case, the first anti-bound state has

$$\kappa_{\min}/\alpha = 0.02179, \quad (4.16)$$

which is small enough to produce a resonance of the scattered wave amplitude $\sin^2 \delta(k)$ at the low energies, as shown in Fig.6(b).

4.2 Spectrum at the IR fixed point

In parameter space, we fix IR boundary conditions at the regions shown in Fig.7, as discussed in Sect.2. In the red and orange patches, we are *forced* to do so by normalizability at $x = 0$. In the yellow patch, we the IR boundary condition is fixed by imposing SUSY. Setting $L = 0$, the S-matrix (4.4) simplifies considerably to

$$S_{\text{IR}}(k) = e^{2i\bar{\delta}} \frac{\Gamma(\frac{1+\nu+\mu-ik/\alpha}{2})\Gamma(\frac{1+\nu-\mu-ik/\alpha}{2})}{\Gamma(\frac{1+\nu+\mu+ik/\alpha}{2})\Gamma(\frac{1+\nu-\mu+ik/\alpha}{2})}. \quad (4.17)$$

Apart from $\bar{\delta}(k)$, the poles of $S_{\text{IR}}(k)$ are at the poles of the pair of Gamma functions in the numerator.

Bound states have $k = i\kappa$, with $\kappa > 0$, so we are searching for the poles of

$$\Gamma\left(\frac{1+\nu+\mu+\kappa/\alpha}{2}\right) \Gamma\left(\frac{1+\nu-\mu+\kappa/\alpha}{2}\right). \quad (4.18)$$

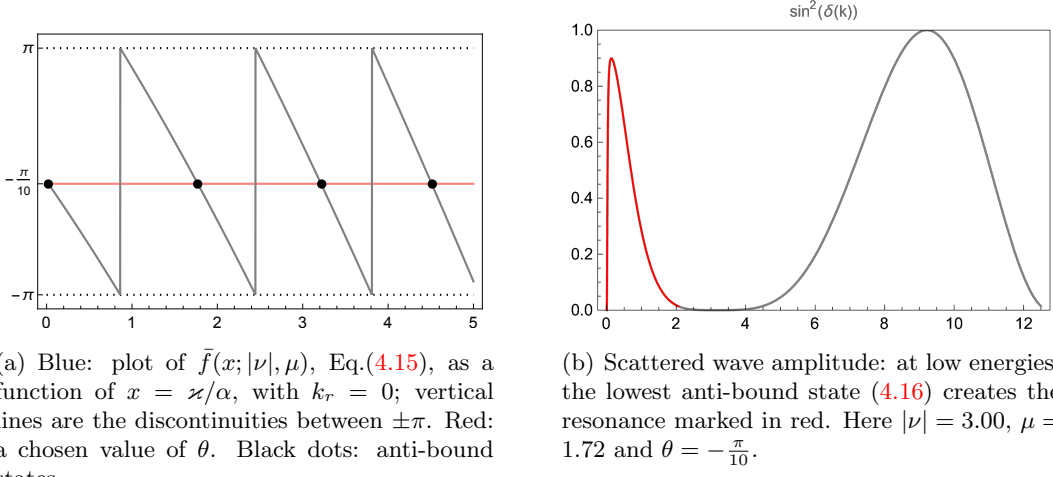


Figure 6

Since here we are assuming $\mu, \nu > 0$, and since $\kappa > 0$, we can only have poles in the second Gamma function, for

$$\kappa_n = \alpha(\mu - \nu - 1 - 2n) > 0, \quad (4.19)$$

where n are non-negative integers. This inequality implies that there is a finite number n_{\max} of bound states, such that

$$0 \leq 2n_{\max} \leq \mu - \nu - 1. \quad (4.20)$$

In turn, (4.20) means that bound states exist, i.e. $n_{\max} > 0$, only if

$$\mu > \nu + 1. \quad (4.21)$$

This condition defines a curve on the g_c - g_s plane, drawn in green in Fig.7, such that we only have bound states in the darker yellow, and darker red patches. In the light red and light yellow patches, where the potential is supersymmetric, the fact that there are no bound states is usually stated as meaning that SUSY is “spontaneously broken”.

Anti-bound states have $k = -i\nu$, with $\nu > 0$. In this case, poles in (4.23) only exist for $\mu > 0$, hence in the range $g_c < \frac{1}{4}$, i.e. the entire red and yellow regions of Fig.7. There are two series of anti-bound modes, corresponding to the poles of each of the Gamma functions in (4.23),

$$\nu_+ = +\mu + \nu + 1 + 2n_+, \quad n_+ = 0, 1, 2, 3, \dots \quad (4.22a)$$

$$\nu_- = -\mu + \nu + 1 + 2n_-, \quad n_- = n_{\min}, n_{\min} + 1, n_{\min} + 2, \dots \quad (4.22b)$$

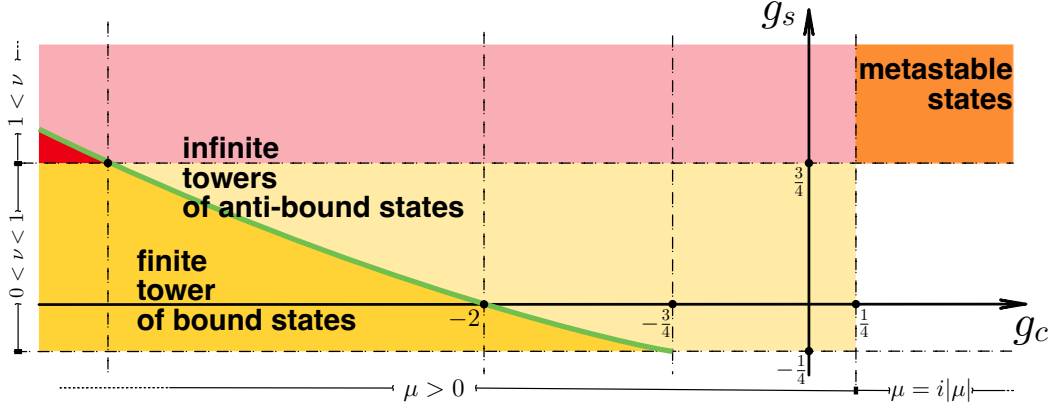


Figure 7: Regions in parameter space where IR boundary conditions can or must be fixed. Metastable states only exist in the orange patch. Bound states exist only in darker yellow, and darker red regions. In the light yellow and light red patches, SUSY is “spontaneously broken”.

In the second series, ν_{\min} is the smallest integer to satisfy the condition $n_{\min} > \mu - \nu - 1$. Note that the “missing” integers $0, 1, \dots, n_{\min} - 1$ are such that $\varkappa_- < 0$; these are just a relabeling of the bound states (4.19). There may be resonances in the series (4.22b). They happens for the small energy values, if $\mu \gtrsim \nu + 1$. We illustrate the presence of one such resonance in Fig.8, a plot of the scattered wave $\sin^2 \delta(k)$. The resonance is the red peak at low k .

For metastable states, we search for poles of the S-matrix with $k = k_r - i\varkappa$ and $k_r \neq 0$, that is, poles of

$$\Gamma\left(\frac{1+\nu+\mu}{2} - \frac{\varkappa + ik_r}{2\alpha}\right) \Gamma\left(\frac{1+\nu-\mu}{2} - \frac{\varkappa + ik_r}{2\alpha}\right). \quad (4.23)$$

At the IR fixed point, we always have real $\nu > 0$. To cancel the ik_r factor, we must have $\mu = i|\mu|$, which means that we must take $g_c > \frac{1}{4}$. In turn, this imposes $g_s > \frac{3}{4}$ so that we remain in the IR fixed point. Hence we are now restricted to the orange region in Fig.7. When all is set, we first see that there are no poles with $\varkappa < 0$ and $k_r \neq 0$, hence no instabilities. There are poles that give a series of metastable states, with

$$k_n = k_r - i\varkappa_n \quad \begin{cases} k_r = \alpha|\mu| \\ \varkappa_n = \alpha(2n + 1 + \nu) \\ n = 0, 1, 2, 3, \dots \end{cases} \quad (4.24)$$

The most stable mode is the one with the smallest imaginary part, i.e. $\varkappa_0 = \alpha(\nu + 1)$,

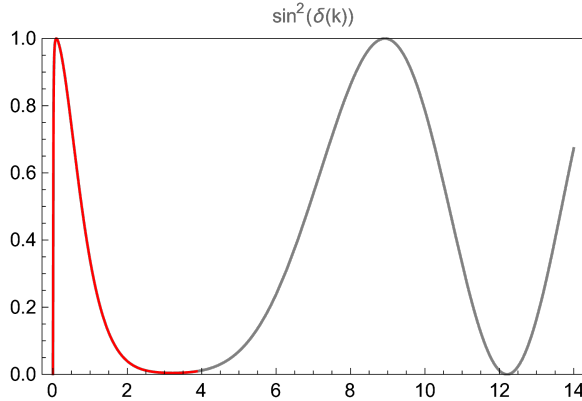


Figure 8: Resonance at low energy due to an anti-bound state with IR boundary conditions; here we choose $\nu = 5.59$ and $\mu = 6.60$.

which has the longest lifetime

$$\tau_0 = \frac{2m/\hbar}{\alpha^2|\mu|(1+\nu)} \quad (4.25)$$

Given that $\nu > 0$, in units of k_r/α , the largest lifetime $\tau_0 \sim 1/(1+\nu)$ is still not large, so these metastable states are not resonances.

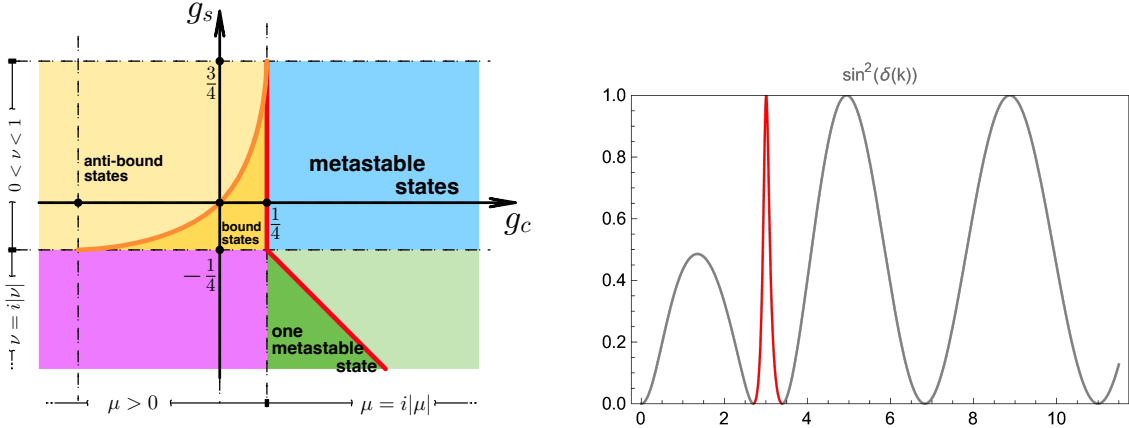
Although we have no special reason for fixing $L = 0$ in the regions of Fig.4, nothing *forbids* us to do so. Searching for poles of $S_{\text{IR}}(k)$ with μ and ν in these regions, we can see that *there are no bound states in the IR fixed point, in any of the three patches shown in Fig.4*. There are anti-bound and metastable states in some parts of these regions, though; the analysis of their existence is analogous to that at the UV fixed point, which we describe below.

4.3 Spectrum at the UV fixed point

Similarly to what happens at the IR fixed point, at the UV point, $L = \infty$, the S-matrix (4.4) drastically simplifies to

$$S_{\text{UV}}(k) = e^{2i\delta} \frac{\Gamma(\frac{1-\nu+\mu-ik/\alpha}{2})\Gamma(\frac{1-\nu-\mu-ik/\alpha}{2})}{\Gamma(\frac{1-\nu+\mu+ik/\alpha}{2})\Gamma(\frac{1-\nu-\mu+ik/\alpha}{2})}. \quad (4.26)$$

As discussed in Sect.2.2, we can only go to the UV fixed point if we are not forced to choose IR boundary conditions. So we must be in one of the patches of Fig.9(a), where at least one of μ or ν is imaginary. Inspection of (4.26) shows that, in this case, *there are no bound states*.



(a) Spectra in regions of parameter space with UV boundary condition. Metastable states become anti-bound states on the red line. There are no bound, anti-bound, nor metastable states in the purple and light green regions.

(b) Plot of scattering amplitude with resonance around $k/\alpha = |\mu|$ marked in red. Here $\nu = 0.9$ and $|\mu| = 3.0$.

Figure 9

To find metastable and anti-bound states, we take $k = k_r - i\kappa$, and search for poles of the Gamma functions in the numerator. First take $\nu = i|\nu|$ and $\mu > 0$, in the purple patch of Fig.9(a); it is impossible to cancel the imaginary parts of the arguments of the Gamma functions, so there are no poles, hence *no anti-bound nor metastable states*.

For $\nu > 0$ real, in the blue patch of Fig.9(a), we want poles of

$$\Gamma\left(\frac{1-\nu+i|\mu|}{2} - \frac{\kappa+ik_r}{2\alpha}\right) \Gamma\left(\frac{1-\nu-i|\mu|}{2} - \frac{\kappa+ik_r}{2\alpha}\right), \quad (4.27)$$

with $k_r > 0$. There are poles of the first Gamma function, at

$$0 < \nu < 1, \quad k_n = k_r - i\kappa_n \quad \begin{cases} k_r = \alpha|\mu| \\ \kappa_n = \alpha(2n+1-\nu) \\ n = 0, 1, 2, 3, \dots \end{cases} \quad (4.28)$$

Since $0 < \nu < 1$, $\kappa > 0$ and the system is stable. Hence we have *metastable states which, at the threshold of the blue region, where $\mu = 0$, become a series of anti-bound states*. The first metastable (or anti-bound) mode has $\kappa_0 = \alpha(1-\nu)$, which becomes arbitrarily small if $\nu \lesssim 1$, i.e. near the threshold $g_s \approx \frac{3}{4}$. In this case, the lifetime $\tau_0 \sim 1/(1-\nu)$ becomes arbitrarily large, creating a resonance, as illustrated in Fig.9(b).

Now take $\nu = i|\nu|$ and $\mu = i|\mu|$, in the green patch of Fig.9(a). We want poles of

$$\Gamma\left(\frac{1+i(|\mu|-|\nu|)}{2} - \frac{\kappa+ik_r}{2\alpha}\right) \Gamma\left(\frac{1-i(|\nu|+|\mu|)}{2} - \frac{\kappa+ik_r}{2\alpha}\right), \quad (4.29)$$

We have one single possible metastable state, a pole of the first Gamma function that exists if $|\mu| - |\nu| > 0$, at

$$|\mu| - |\nu| > 0, \quad k = k_r - i\kappa \quad \begin{cases} k_r = \alpha(|\mu| - \nu) \\ \kappa = \alpha \end{cases} \quad (4.30)$$

In parameter space, the condition $|\mu| > |\nu|$ gives a triangular region, the dark green patch in Fig.9(a). On the border of this region given by the diagonal line $|\mu| = |\nu|$, the single metastable state (4.30) becomes one single anti-bound state,

$$|\mu| = |\nu|, \quad k = -i\kappa, \quad \kappa = \alpha. \quad (4.31)$$

The medium-weak region

We have found the metastable modes (4.28) in the blue patch of the medium-weak region, where $g_c > \frac{1}{4}$. The other half, where $g_c < \frac{1}{4}$, is the yellow patch of Fig.9(a). Here the potential is supersymmetric, and we used SUSY to fix $L = 0$ as in its superpartner strongly-coupled region. But we are not actually *forbidden* of setting $L \neq 0$, and, in particular we are allowed to set $L = \infty$. Now μ and ν are both real, and the poles of $S_{UV}(k)$ with $k = i\kappa$ are the poles of

$$\Gamma\left(\frac{1 - \nu + \mu + \kappa/\alpha}{2}\right)\Gamma\left(\frac{1 - \nu - \mu + \kappa/\alpha}{2}\right).$$

Since $0 < \nu < 1$, there are only poles at the second Gamma function. Thus we have *a finite tower of bound states*, with the $\kappa_n > 0$

$$\kappa_n = \alpha(\mu + \nu - 1 - 2n), \quad n \in \mathbb{N}, \quad (4.32)$$

having a maximum mode n_{\max} such that

$$0 \leq 2n_{\max} \leq \mu + \nu - 1. \quad (4.33)$$

Imposing that $n_{\max} \geq 0$ gives a restriction in the g_c - g_s plane in terms of a curve $\mu = -\nu + 1$, drawn in orange in Fig.9(a). Compare these to Eqs.(4.19)-(4.21), for bound states in the same region in parameter space, but in the IR fixed point of the RG flow. Here, we can again find two series of anti-bound states analogous to (4.22) and, as in the IR case, no metastable states.

4.4 Completing the spectrum in the medium-weak region

In the medium-weak region of parameter space, we can extend the spectrum of the Pöschl-Teller potential over the singularity at $x = 0$, to functions defined on the entire real line. This is equivalent to a self-adjoint extension of the Hamiltonian, but here done under the interpretation of the renormalization group.

To illustrate the procedure clearly, consider first consider a special case. The medium-weak region of parameter space, where the boundary conditions are *not* fixed by normalizability at $x = 0$, contains the line

$$g_s = 0 \quad \text{hence} \quad \nu = \frac{1}{2}, \quad (4.34)$$

and g_c arbitrary. For $\nu = \frac{1}{2}$, Eq.(3.6) becomes

$$\psi'_k(R) - \frac{1}{R + \varepsilon L} \psi_k(R) = 0, \quad (4.35)$$

which has a well-defined $R \rightarrow 0$ limit,

$$\psi'_k(0) - \frac{\varepsilon}{L} \psi_k(0) = 0, \quad (4.36)$$

so the Robin boundary conditions can be transferred directly to the origin, with no need for a cutoff. The IR fixed point, $L = 0$, gives the Dirichlet condition $\psi_k(0) = 0$, while the UV fixed point, $L = \infty$, gives the Neumann condition $\psi'_k(0) = 0$. Inside the weak-medium region of coupling space, we might be interested in changing g_s (say, adiabatically) without changing the boundary conditions. Then chosing the UV and the IR fixed points imply, respectively, the choice of Neumann or Dirichlet boundary conditions.

On the line (4.34), the Pöschl-Teller potential is not singular at the origin, it degenerates into

$$\mathcal{V}_0(x) = \frac{\alpha^2 g_c}{\cosh^2(\alpha x)}, \quad (4.37)$$

which has no singularity, and is well-defined for all $x \in \mathbb{R}$ in the entire real line. The spectrum is well-known. For $g_c < 0$, we have a finite tower of bound states with $k_N = i\kappa_N$,

$$\kappa_N = \alpha(\mu - \frac{1}{2} - N) > 0, \quad N \in \mathbb{Z}_{\geq 0}. \quad (4.38)$$

We thus have bound states with both odd and even N , corresponding to the two well-defined parities of the eigenstates of the symmetric potential $\mathcal{V}_0(x) = \mathcal{V}_0(-x)$.

Now, if we take the limit $g_s \rightarrow 0$, hence $\nu \rightarrow \frac{1}{2}$, in the spectrum obtained in Eq.(4.19), we do find (4.38), but *only the odd modes* $N = 2n + 1$. What happens is that, to get to (4.19), we had fixed the IR boundary conditions consistent with SUSY, which amounts to imposing a Dirichlet condition at the origin, $\psi(0) = 0$, and this condition only holds for the odd-parity states of the symmetric potential \mathcal{V}_0 . The even-parity states of \mathcal{V}_0 , with $N = 2n$ are those that satisfy the Neumann condition $\psi'(0) = 0$ instead. These even states can also be found in our renormalization scheme, but they are at the UV fixed point of the RG flow. Indeed, setting $\nu = \frac{1}{2}$ in the UV bound states (4.32), we find $\kappa_n = \alpha(\mu - \frac{1}{2} - 2n)$, which are precisely the even modes, $N = 2n$, in (4.38).

To summarize: to find all the eigenstates of the degenerate potential (4.37), *we must use two independent renormalization scales L_{IR} and L_{UV} , and set one of them to the IR, $L_{\text{IR}} = 0$, and the other to the UV, $L_{\text{UV}} = \infty$.*⁵

The procedure above can be used to extend the eigenfunctions of the Pöschl-Teller potential, not only in the degenerate case $g_s = 0$, but on all of the medium-weak region in parameter space. Bound states with odd modes κ_n^- are given by the poles of $S_{\text{IR}}(\kappa)$, and those with even modes κ_n^+ by the poles of $S_{\text{UV}}(\kappa)$, which were all found in (4.19) and (4.32). Thus the spectrum of bound states for medium-weak potentials extended to the entire real line is

$$\kappa_n^\pm = \alpha(\mu \pm \nu - 2n - 1), \quad n \in \mathbb{N}, \quad (4.39)$$

with contributions from both fixed points.

5 Conclusion

In this paper, we have used a renormalization procedure to obtain well-defined energy eigenfunctions of the Pöschl-Teller potential on the entire parameter plane g_s - g_c , including the regions where the singularity at the origin renders the boundary conditions non-trivial. Renormalization introduces a length scale L by dimensional transmutation, which parameterizes the family of solutions of the Schrödinger equation. In the strongly attractive region, the scale L is replaced by a phase θ .

The renormalization group is complicated, with L competing with the intrinsic length scale of the potential, $1/\alpha$, for the breaking of asymptotic conformal symmetry near the origin. We studied how the beta function and the running coupling behave in different patches of the g_s - g_c plane. Near the singularity, for finite L , the beta function is asymptotically the same as that of the conformal potential, with two fixed points, but the IR point is unreachable because conformal symmetry eventually is explicitly broken. When we cross the line from the medium-weak to the strongly attractive regions of parameter space, the two fixed points merge, undergo a BKT phase transition, then disappear. For $L = 0$ and for $L = \infty$, there is a radical change in the beta function and running coupling, which are driven exclusively by the explicit breaking of conformal symmetry induced by $1/\alpha$. We have been able to compute the beta function perturbatively in these cases.

In the strongly repulsive region of parameter space, the scale L must be set to vanish by the normalizability of the wave function. We have shown that in the patch of the medium-weak region where the Pöschl-Teller potential is supersymmetric, SUSY can be used to fix $L = 0$ and prevent spontaneous breaking of asymptotic conformal symmetry, a phenomenon analogous to the one described by some of the present authors in [25] for the exactly conformal potential.

⁵A similar approach was used in [32] to find the spectrum on the entire real line of the harmonic oscillator added of a term $\sim 1/x^2$. The authors impose a small cutoff to the superpotential, which generates a delta-function spike to the potential, providing an explicit representation of the regularization procedure.

Finally, from the wave functions, we computed the S-matrix in all regions of parameter space, and classified the stable, metastable and bound states. The spectrum depends on the value of the anomalous dimension L or the phase θ , as was to be expected.

Our results might be useful in the contexts of several known applications of the Pöschl-Teller potential, such as fluctuations of relativistic models [5–10], and of black holes [11–16]. For example, in the context of quasinormal modes, a discussion of the self-adjoint extensions of the Pöschl-Teller potential has recently been made in [13, 14], with an approach different from ours.

One possible extension of the present work would be applying the renormalization framework to other potentials with an inverse-square singularity, in particular those that, like the Pöschl-Teller potential, are supersymmetric and shape-invariant [27], including the class of potentials constructed in [33–36]. Note that all the shape-invariant potentials which are independent of \hbar have been classified, and those which are restricted to half the real line because of the existence of a singularity all diverge as $\sim g/x^2$, see [27]. These potentials might have uses in the study of fluctuations of naked singularities [14, 37].

The explicit breaking of conformal symmetry is a general feature of all potentials which are not conformal, but have an inverse-square singularity and hence asymptotic conformal symmetry. It would be interesting to apply our construction of the RG flow to these cases.

It would also be interesting to understand whether the RG flow described here could have some holographical interpretation in terms of asymptotically AdS spaces, as the Robin boundary conditions that we have found in the course of the renormalization procedure are the same that appear in [15, 16].

Finally, it would be interesting to consider the trigonometric version of the Pöschl-Teller potential, which, in place of the hyperbolic functions have a sine and a cosine. This potential describes a unidimensional Bravais lattice. In this case, when present, SUSY trivializes the lattice structure and does not allow energy bands [38]. But in the regions of parameter space where there is no SUSY, renormalization should introduce a family with an infinite number of parameters. We believe that these could be fixed to generate Bloch boundary conditions and non-trivial lattice structures.

Acknowledgments

AAL and UCdS would like to thank GM Sotkov for stimulating conversation. CFSP is funded by CAPES.

A α -corrections to the running coupling

In this appendix, we show what happens to the RG flow if we consider a perturbative expansion in powers of αR . As stated in (3.8), this is a small, dimensionless number. It

measures the cutoff R against the Pöschl-Teller intrinsic length scale $1/\alpha$. Taking αR as small, but not zero, shows how this scale $1/\alpha$ affects the RG flow.

If we compute the running coupling $\gamma(R)$ with ψ_0 , from the solution (2.4), we can organize the result as

$$\gamma(R) = \nu \frac{1 - \varepsilon(L/R)^{2\nu} + \sum_{n=1}^{\infty} [N_n^0 + \tilde{N}_n^0 \varepsilon(L/R)^{2\nu}] (\alpha R)^{2n}}{1 + \varepsilon(L/R)^{2\nu} + \sum_{n=1}^{\infty} [D_n^0 + \tilde{D}_n^0 \varepsilon(L/R)^{2\nu}] (\alpha R)^{2n}} \quad (\text{A.1})$$

where ε and L are defined in (3.10) and (3.11), and the coefficients N_n^0 , \tilde{N}_n^0 , D_n^0 , \tilde{D}_n^0 are dimensionless constants depending only on μ , ν .

Now let us compute the equivalent of the r.h.s. of Eq.(3.7) using $\psi_k(x)$ with $k > 0$ instead of $\psi_0(x)$. Since x and k always appear in the dimensionless combinations αx and k/α in the solution (2.4), we find that

$$-\frac{1}{2} + R \frac{\psi'_k(R)}{\psi_k(R)} = \nu \frac{1 - \frac{A_k}{B_k} R^{2\nu} + \sum_{n=1}^{\infty} [N_n(k) + \tilde{N}_n(k) \frac{A_k}{B_k} R^{2\nu}] (\alpha R)^{2n}}{1 + \frac{A_k}{B_k} R^{2\nu} + \sum_{n=1}^{\infty} [D_n(k) + \tilde{D}_n(k) \frac{A_k}{B_k} R^{2\nu}] (\alpha R)^{2n}} \quad (\text{A.2})$$

where the series' coefficients are polynomials in k/α , of the form

$$\begin{aligned} N_n(k) &= N_n^0 + \sum_{j=1}^{2n} n_j (k/\alpha)^j, & \tilde{N}_n(k) &= \tilde{N}_n^0 + \sum_{j=1}^{2n} \tilde{n}_j (k/\alpha)^j, \\ D_n(k) &= D_n^0 + \sum_{j=1}^{2n} d_j (k/\alpha)^j, & \tilde{D}_n(k) &= \tilde{D}_n^0 + \sum_{j=1}^{2n} \tilde{d}_j (k/\alpha)^j, \end{aligned} \quad (\text{A.3})$$

with n_j , \tilde{n}_j , d_j , \tilde{d}_j being dimensionless constants that do not depend on k . The highest power of k in each term of the series in (A.2) matches the corresponding power of R .⁶ So we have at least one factor of αR for each factor of k/α and, when the condition (3.2) for an effective description of the singularity is imposed, we get

$$-\frac{1}{2} + R \frac{\psi'_k(R)}{\psi_k(R)} = \nu \frac{1 - \frac{A_k}{B_k} R^{2\nu} + \sum_{n=1}^{\infty} [N_n^0 + \tilde{N}_n^0 \frac{A_k}{B_k} R^{2\nu}] (\alpha R)^{2n}}{1 + \frac{A_k}{B_k} R^{2\nu} + \sum_{n=1}^{\infty} [D_n^0 + \tilde{D}_n^0 \frac{A_k}{B_k} R^{2\nu}] (\alpha R)^{2n}} \quad \text{for } kR \ll 1. \quad (\text{A.4})$$

Now, while $kR \ll 1$, Eq.(3.6) implies that the r.h.s. of Eqs.(A.4) and (3.7) must match. The only way for this to happen is if $A_k/B_k = \varepsilon L^{2\nu}$, as stated in Eq.(3.12). More specifically, taking only zero order terms in αR , we find

$$-\frac{1}{2} + R \frac{\psi'_k(R)}{\psi_k(R)} = \nu \frac{1 - \frac{B_k}{A_k} R^{-2\nu}}{1 + \frac{A_k}{B_k} R^{-2\nu}} \quad (\text{A.5})$$

which must match the running coupling (3.9), and we arrive again at Eq.(3.12).

⁶This can be seen by noting that k/α only appears in the arguments a and b of the hypergeometrics ${}_2F_1(a, b; c; z)$; the power of k then matches the powers of ab in the Pochhammer symbols.

B The critical line $g_s = -\frac{1}{4}$

On the line in parameter space defined by $g_s = -\frac{1}{4}$, we have $\nu = 0$, and the second solution of the hypergeometric equation appearing in (2.4) is not valid, due to a logarithmic branch of Eq.(2.3) at the origin. A second solution can then be given by an hypergeometric centered at some other singularity, e.g. at $u = 1$. Thus, the function

$$[\tanh(\alpha x)]^{\frac{1}{2}} [\cosh(\alpha x)]^{-i\frac{k}{\alpha}} {}_2F_1 \left[\frac{1-\mu+ik/\alpha}{2}, \frac{1+\mu+ik/\alpha}{2}; 1 + \frac{ik}{\alpha}; \frac{1}{\cosh^2(\alpha x)} \right] \quad (\text{B.1})$$

is a solution of (2.3) for $\nu = 0$; see e.g. [30, §15]. This is a complex function, whose complex conjugate is also a solution of (2.3). Since we want a real solution, we combine both, and take the real part of (B.1) as the second linearly independent solution of (2.3) when $\nu = 0$. Thus the general wave function in this case reads

$$\begin{aligned} \psi_k(x) = & \frac{[\tanh(\alpha x)]^{\frac{1}{2}}}{\alpha^{\frac{1}{2}}} \left[\mathcal{A}_k [\cosh(\alpha x)]^{-i\frac{k}{\alpha}} {}_2F_1 \left(\frac{1-\mu+ik/\alpha}{2}, \frac{1+\mu+ik/\alpha}{2}; 1; \tanh^2(\alpha x) \right) \right. \\ & + \frac{\mathcal{B}_k}{2} \left([\cosh(\alpha x)]^{-\frac{ik}{\alpha}} \frac{\Gamma(\frac{1-\mu+ik/\alpha}{2})\Gamma(\frac{1+\mu+ik/\alpha}{2})}{\Gamma(1+\frac{ik}{\alpha})} {}_2F_1 \left(\frac{1-\mu+ik/\alpha}{2}, \frac{1+\mu+ik/\alpha}{2}; 1 + \frac{ik}{\alpha}; \frac{1}{\cosh^2(\alpha x)} \right) \right. \\ & \left. \left. + [\cosh(\alpha x)]^{\frac{ik}{\alpha}} \frac{\Gamma(\frac{1-\mu-ik/\alpha}{2})\Gamma(\frac{1+\mu-ik/\alpha}{2})}{\Gamma(1-\frac{ik}{\alpha})} {}_2F_1 \left(\frac{1-\mu-ik/\alpha}{2}, \frac{1+\mu-ik/\alpha}{2}; 1 - \frac{ik}{\alpha}; \frac{1}{\cosh^2(\alpha x)} \right) \right) \right] \end{aligned} \quad (\text{B.2})$$

The factors of Gamma functions were chosen such that, expanding the hypergeometrics near the origin we find

$$\psi_k(x) \approx \mathcal{C}_k x^{1/2} \left[1 - \frac{\mathcal{B}_k}{\mathcal{C}_k} \log(\alpha x) \right], \quad (\text{B.3})$$

where

$$\mathcal{C}_k \equiv \mathcal{A}_k - \mathcal{B}_k \left[2\gamma + \text{Re} \left[\psi^{(0)} \left(\frac{1-\mu+ik/\alpha}{2} \right) + \psi^{(0)} \left(\frac{1+\mu+ik/\alpha}{2} \right) \right] \right] \quad (\text{B.4})$$

with γ the Euler-Mascheroni constant and $\psi^{(0)}(z)$ the digamma function [30, §5]. The asymptotic expansion at infinity is a combination of ingoing and outgoing waves,

$$\begin{aligned} \psi_k(x) \approx & \frac{1}{\alpha^{\frac{1}{2}}} \left[\frac{\Gamma(\frac{ik}{\alpha}) \mathcal{A}_k}{\Gamma(\frac{1+\mu+ik/\alpha}{2})\Gamma(\frac{1-\mu+ik/\alpha}{2})} + \frac{\Gamma(\frac{1-\mu-ik/\alpha}{2})\Gamma(\frac{1+\mu-ik/\alpha}{2}) \mathcal{B}_k}{\Gamma(1-\frac{ik}{\alpha})} \frac{2}{2} \right] \frac{e^{ikx}}{2^{\frac{2ik}{\alpha}}} \\ & + \text{Complex Conjugate} \end{aligned} \quad (\text{B.5})$$

Renormalization

Using the asymptotic solution (B.3) with $k = 0$, we can compute $\mathcal{F}(R)$, cf. Eq.(3.6),

$$R\mathcal{F}(R) = \frac{1}{2} - \frac{\mathcal{D}}{1 - \mathcal{D} \log(\alpha R)}, \quad (\text{B.6})$$

with

$$\mathcal{D} = \mathcal{B}_0/\mathcal{C}_0 = \mathcal{B}_k/\mathcal{C}_k \quad (\text{B.7})$$

independent of k . Using Eq.(B.4) we can write this as a relation between \mathcal{A}_k and \mathcal{B}_k ,

$$\frac{\mathcal{A}_k}{\mathcal{B}_k} = \frac{1}{2} \left[\psi^{(0)} \left(\frac{1-\mu+ik/\alpha}{2} \right) + \psi^{(0)} \left(\frac{1+\mu+ik/\alpha}{2} \right) + \text{C.C.} \right] + \frac{1}{\mathcal{D}} + 2\gamma. \quad (\text{B.8})$$

Spectrum at the fixed point

Choosing $\mathcal{B}_k = 0$ is necessary when $g_c < 1/4$, i.e. μ is real. In this case, Eq.(B.5) simplifies. In terms of the phase shift, we have the S-matrix $S(k) = e^{2i\delta(k)}$ given by

$$S_0(k) = -\frac{\Gamma(\frac{ik}{\alpha})\Gamma(\frac{1}{2} + \frac{\mu}{2} - \frac{ik}{2\alpha})\Gamma(\frac{1}{2} - \frac{\mu}{2} - \frac{ik}{2\alpha})}{\Gamma(-\frac{ik}{\alpha})\Gamma(\frac{1}{2} + \frac{\mu}{2} + \frac{ik}{2\alpha})\Gamma(\frac{1}{2} - \frac{\mu}{2} + \frac{ik}{2\alpha})}. \quad (\text{B.9})$$

This result is valid even for imaginary μ ($g_c > \frac{1}{4}$). From the S-matrix we find the bound, anti-bound and metastable states to be, respectively,

$$\kappa_n = \alpha(\mu - 2n - 1), \quad n = 0, 1, 2, 3, \dots \quad (\text{B.10})$$

$$\kappa_{n\pm}^{\text{AB}} = \alpha(2n_{\pm} \pm \mu + 1), \quad \begin{cases} n_+ = 0, 1, 2, 3, \dots \\ n_- = n_-^{\min}, n_-^{\min} + 1, \dots \end{cases} \quad (\text{B.11})$$

$$k_n^{\text{MS}} = \alpha[|\mu| - i(2n + 1)], \quad n = 0, 1, 2, 3, \dots \quad (\text{B.12})$$

where n_-^{\min} is the first integer to satisfy the inequality $2n_-^{\min} > \mu - 1$. Bound states exist for $g_c < -\frac{3}{4}$ ($\mu > 1$); metastable states for $g_c > \frac{1}{4}$ ($\mu = i|\mu|$); anti-bound states for $g_c < \frac{1}{4}$ ($\mu > 0$). The poles of metastable states cannot get arbitrarily close to the real axis, and do not create resonances. When $\mu \approx 1$, $g_c \approx -\frac{3}{4}$, we have a strong resonance at low energies, created by the bound state if $\mu > 1$ or by the anti-bound state if $\mu < 1$. These results correspond to the limit $\nu \rightarrow 0$ of the spectra computed at the two fixed points L_{IR} and L_{UV} in the main text. The bound and anti-bound states correspond to the IR fixed point, Eqs. (4.19), (4.22a) and (4.22b), and the metastable states are given by the UV fixed point, Eq.(4.28).

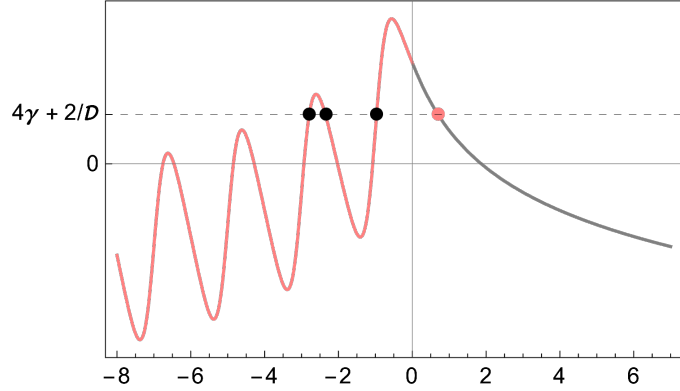


Figure 10: Plot of $\mathcal{F}_0(x; i|\mu|)$ as a function of $x = \kappa/\alpha$. The horizontal line is a given value of $4\gamma + 2/\mathcal{D}$. Anti-bound states exist at the intersections when $\kappa < 0$, and bound states at the intersection when $\kappa > 0$.

Spectra outside the fixed point

To be outside the fixed point, we must have $g_c > 1/4$, hence $\mu = i|\mu|$. The asymptotic solution (B.5) gives the S-matrix

$$S_{L_0}(k) = S_0(k) \left[\frac{2\mathcal{A}(k)}{\mathcal{B}(k)} + \frac{i\alpha}{k} \frac{\left| \Gamma\left(\frac{1-i|\mu|-ik/\alpha}{2}\right) \right|^2 \left| \Gamma\left(\frac{1+i|\mu|-ik/\alpha}{2}\right) \right|^2}{\left| \Gamma\left(\frac{ik}{\alpha}\right) \right|^2} \right]^{-1} \times \left[\frac{2\mathcal{A}(k)}{\mathcal{B}(k)} - \frac{i\alpha}{k} \frac{\left| \Gamma\left(\frac{1-i|\mu|-ik/\alpha}{2}\right) \right|^2 \left| \Gamma\left(\frac{1+i|\mu|-ik/\alpha}{2}\right) \right|^2}{\left| \Gamma\left(\frac{ik}{\alpha}\right) \right|^2} \right]^{-1} \quad (\text{B.13})$$

Here we used that $\Gamma(1+x) = x\Gamma(x)$, and $2\mathcal{A}(k)/\mathcal{B}(k)$ is given by (B.8) in terms of the length scale (3.27) defined by \mathcal{D} . We have factorized the S-matrix at the fixed point $S(k)$, given by Eq.(B.9). Since the poles of $S_0(k)$ are not poles of the new factor in $S_{L_0}(k)$, the metastable states (B.12) are poles of $S_{L_0}(k)$, so they still exist outside the fixed point. The new poles are the solutions of

$$\frac{2}{\mathcal{D}} + 4\gamma = \mathcal{F}_0(k/\alpha; i|\mu|), \quad (\text{B.14})$$

where

$$\begin{aligned} \mathcal{F}_0(k/\alpha; i|\mu|) &\equiv \frac{\alpha}{\kappa} \frac{\Gamma\left(\frac{1-i|\mu|-ik/\alpha}{2}\right) \Gamma\left(\frac{1-i|\mu|+ik/\alpha}{2}\right) \Gamma\left(\frac{1+i|\mu|-ik/\alpha}{2}\right) \Gamma\left(\frac{1+i|\mu|+ik/\alpha}{2}\right)}{\Gamma\left(-\frac{ik}{\alpha}\right) \Gamma\left(\frac{ik}{\alpha}\right)} \\ &\quad - \left[\psi^{(0)}\left(\frac{1-\mu+ik/\alpha}{2}\right) + \psi^{(0)}\left(\frac{1+\mu+ik/\alpha}{2}\right) \psi^{(0)}\left(\frac{1-\mu-ik/\alpha}{2}\right) + \psi^{(0)}\left(\frac{1+\mu-ik/\alpha}{2}\right) \right]. \end{aligned}$$

Depending on the value of \mathcal{D} , we may have no bound nor anti-bound states; up to two anti-bound states and no bound state; or a finite number of anti-bound states and one bound state. In Fig.10 we have a typical curve of $\mathcal{F}_0(k/\alpha; i|\mu|)$; the bound and anti-bound states are the points where the curve touches the horizontal line $2/\mathcal{D} + 4\gamma$. In the example shown, there are three anti-bound states (black dots), and one bound state (red dot). Finally, by direct inspection it is easy to see that there are no metastable states, since the right-hand-side of Eq.(B.14) is complex for $k = k_r - i\kappa$.

References

- [1] G. Pöschl and E. Teller, “Bemerkungen zur Quantenmechanik des anharmonischen Oszillators,” *Z. Phys.* **83** (1933) 143–151.
- [2] V. de Alfaro, S. Fubini, and G. Furlan, “Conformal Invariance in Quantum Mechanics,” *Nuovo Cim. A* **34** (1976) 569.
- [3] F. Calogero, “Solution of the one-dimensional N body problems with quadratic and/or inversely quadratic pair potentials,” *J. Math. Phys.* **12** (1971) 419–436.
- [4] D. M. Gitman, I. V. Tyutin, and B. L. Voronov, “Self-adjoint extensions and spectral analysis in Calogero problem,” [arXiv:0903.5277 \[quant-ph\]](https://arxiv.org/abs/0903.5277).
- [5] T. S. Mendonça and H. P. de Oliveira, “A note about a new class of two-kinks,” *Journal of High Energy Physics* **2015** (2015) no. 6, 1–12.
- [6] T. S. Mendonça and H. P. de Oliveira, “The collision of two-kinks defects,” *JHEP* **09** (2015) 120, [arXiv:1502.03870 \[hep-th\]](https://arxiv.org/abs/1502.03870).
- [7] T. S. Mendonça and H. D. Oliveira, “The collision of two-kinks revisited: the creation of kinks and lump-like defects as metastable states,” *Brazilian Journal of Physics* **49** (2019) no. 6, 914–922.
- [8] Y. Zhong, “Singular Pöschl–Teller II potentials and gravitating kinks,” *JHEP* **09** (2022) 165, [arXiv:2207.12681 \[hep-th\]](https://arxiv.org/abs/2207.12681).
- [9] D. Bazeia, J. a. G. F. Campos, and A. Mohammadi, “Resonance mediated by fermions in kink-antikink collisions,” *JHEP* **12** (2022) 085, [arXiv:2208.13261 \[hep-th\]](https://arxiv.org/abs/2208.13261).
- [10] D.-P. Du, B. Wang, and R.-K. Su, “Quasinormal modes in pure de Sitter space-times,” *Phys. Rev. D* **70** (2004) 064024, [arXiv:hep-th/0404047](https://arxiv.org/abs/hep-th/0404047).
- [11] E. Berti, V. Cardoso, and A. O. Starinets, “Quasinormal modes of black holes and black branes,” *Class. Quant. Grav.* **26** (2009) 163001, [arXiv:0905.2975 \[gr-qc\]](https://arxiv.org/abs/0905.2975).

- [12] R. A. Konoplya and A. Zhidenko, “Quasinormal modes of black holes: From astrophysics to string theory,” *Rev. Mod. Phys.* **83** (2011) 793–836, [arXiv:1102.4014 \[gr-qc\]](https://arxiv.org/abs/1102.4014).
- [13] A. F. Cardona and C. Molina, “Quasinormal modes of generalized Pöschl–Teller potentials,” *Class. Quant. Grav.* **34** (2017) no. 24, 245002, [arXiv:1711.00479 \[gr-qc\]](https://arxiv.org/abs/1711.00479).
- [14] J. C. Fabris, M. G. Richarte, and A. Saa, “Quasinormal modes and self-adjoint extensions of the Schrödinger operator,” *Phys. Rev. D* **103** (2021) no. 4, 045001, [arXiv:2010.10674 \[gr-qc\]](https://arxiv.org/abs/2010.10674).
- [15] T. Harada, T. Ishii, T. Katagiri, and N. Tanahashi, “Hairy black holes in AdS with Robin boundary conditions,” [arXiv:2304.02267 \[hep-th\]](https://arxiv.org/abs/2304.02267).
- [16] S. Kinoshita, T. Kozuka, K. Murata, and K. Sugawara, “Quasinormal mode spectrum of the AdS black hole with the Robin boundary condition,” [arXiv:2305.17942 \[gr-qc\]](https://arxiv.org/abs/2305.17942).
- [17] H. E. Camblong, L. N. Epele, H. Fanchiotti, and C. A. Garcia Canal, “Renormalization of the inverse square potential,” *Phys. Rev. Lett.* **85** (2000) 1590–1593, [arXiv:hep-th/0003014](https://arxiv.org/abs/hep-th/0003014).
- [18] H. E. Camblong and C. R. Ordóñez, “Renormalization in conformal quantum mechanics,” *Phys. Lett. A* **345** (2005) 22–30, [arXiv:hep-th/0305035](https://arxiv.org/abs/hep-th/0305035).
- [19] D. B. Kaplan, J.-W. Lee, D. T. Son, and M. A. Stephanov, “Conformality Lost,” *Phys. Rev. D* **80** (2009) 125005, [arXiv:0905.4752 \[hep-th\]](https://arxiv.org/abs/0905.4752).
- [20] S. R. Beane, P. F. Bedaque, L. Childress, A. Kryjevski, J. McGuire, and U. van Kolck, “Singular potentials and limit cycles,” *Phys. Rev. A* **64** (2001) 042103, [arXiv:quant-ph/0010073](https://arxiv.org/abs/quant-ph/0010073).
- [21] E. Braaten and D. Phillips, “The Renormalization group limit cycle for the $1/r^2$ potential,” *Phys. Rev. A* **70** (2004) 052111, [arXiv:hep-th/0403168](https://arxiv.org/abs/hep-th/0403168).
- [22] D. Bouaziz and M. Bawin, “Singular inverse-square potential: renormalization and self-adjoint extensions for medium to weak coupling,” *Physical Review A* **89** (2014) no. 2, 022113.
- [23] H. E. Camblong, L. N. Epele, H. Fanchiotti, and C. A. Garcia Canal, “Dimensional transmutation and dimensional regularization in quantum mechanics. 1. General theory,” *Annals Phys.* **287** (2001) 14–56, [arXiv:hep-th/0003255](https://arxiv.org/abs/hep-th/0003255).
- [24] U. Camara da Silva, “Renormalization group flow of the Aharonov-Bohm scattering amplitude,” *Annals Phys.* **398** (2018) 38–54.

- [25] J. V. S. Scursulim, A. A. Lima, U. C. da Silva, and G. M. Sotkov, “Supersymmetry shielding the scaling symmetry of conformal quantum mechanics,” *Phys. Rev. A* **101** (Mar, 2020) 032105, [arXiv:1912.13014 \[hep-th\]](https://arxiv.org/abs/1912.13014).
- [26] F. Cooper, A. Khare, and U. Sukhatme, “Supersymmetry and quantum mechanics,” *Phys. Rept.* **251** (1995) 267–385, [arXiv:hep-th/9405029](https://arxiv.org/abs/hep-th/9405029).
- [27] R. Dutt, A. Khare, and U. P. Sukhatme, “Supersymmetry, Shape Invariance and Exactly Solvable Potentials,” *Am. J. Phys.* **56** (1988) 163–168.
- [28] V. L. Berezinsky, “Destruction of Long-range Order in One-dimensional and Two-dimensional Systems Possessing a Continuous Symmetry Group. II. Quantum Systems.,” *Sov. Phys. JETP* **34** (1972) no. 3, 610.
- [29] V. L. Berezinsky, “Destruction of Long-range Order in One-dimensional and Two-dimensional Systems Having a continuous symmetry group. I. Classical systems,” *Sov. Phys. JETP* **32** (1971) 493–500.
- [30] “NIST Digital Library of Mathematical Functions.” <https://dlmf.nist.gov/>, release 1.1.10 of 2023-06-15. <https://dlmf.nist.gov/>. F. W. J. Olver, A. B. Olde Daalhuis, D. W. Lozier, B. I. Schneider, R. F. Boisvert, C. W. Clark, B. R. Miller, B. V. Saunders, H. S. Cohl, and M. A. McClain, eds.
- [31] V. N. Efimov, “Weakly bound states of three resonantly interacting particles.,” tech. rep., Ioffe Inst. of Physics and Tech., Leningrad, 1970.
- [32] A. Gangopadhyaya, J. V. Mallow, and C. Rasinariu, *Supersymmetric Quantum Mechanics: An Introduction*. World Scientific, 2017.
- [33] S. Odake and R. Sasaki, “Infinitely many shape invariant potentials and new orthogonal polynomials,” *Phys. Lett. B* **679** (2009) 414–417, [arXiv:0906.0142 \[math-ph\]](https://arxiv.org/abs/0906.0142).
- [34] S. Odake and R. Sasaki, “Exactly Solvable Quantum Mechanics and Infinite Families of Multi-indexed Orthogonal Polynomials,” *Phys. Lett. B* **702** (2011) 164–170, [arXiv:1105.0508 \[math-ph\]](https://arxiv.org/abs/1105.0508).
- [35] S. Odake and R. Sasaki, “Infinitely many shape invariant potentials and cubic identities of the Laguerre and Jacobi polynomials,” *J. Math. Phys.* **51** 053513, [arXiv:0911.1585 \[math-ph\]](https://arxiv.org/abs/0911.1585).
- [36] J. Bougie, A. Gangopadhyaya, and J. V. Mallow, “Generation of a Complete Set of Supersymmetric Shape Invariant Potentials from an Euler Equation,” *Phys. Rev. Lett.* **105** (2010) 210402, [arXiv:1008.2035 \[hep-th\]](https://arxiv.org/abs/1008.2035).

- [37] C. Chirenti, A. Saa, and J. Skakala, “Quasinormal modes for the scattering on a naked Reissner-Nordstrom singularity,” *Phys. Rev. D* **86** (2012) 124008, [arXiv:1206.0037 \[gr-qc\]](https://arxiv.org/abs/1206.0037).
- [38] F. Cooper, A. Khare, and U. Sukhatme, *Supersymmetry in Quantum Mechanics*. World Scientific, 2001.